Master's thesis

NTNU
Norwegian University of Science and Technology
Faculty of Natural Sciences
Department of Biology

Ingeborg Skaar Dale

Composition and trophic interactions of the planktonic community in northern Baffin Bay

Master's thesis in Ocean Resources
Supervisor: Maja Hatlebakk
Co-supervisor: Glaucia Fragoso and Geir Johnsen
May 2024

NTNU
Norwegian University of
Science and Technology

Ingeborg Skaar Dale

Composition and trophic interactions of the planktonic community in northern Baffin Bay

Master's thesis in Ocean Resources
Supervisor: Maja Hatlebakk
Co-supervisor: Glaucia Fragoso and Geir Johnsen
May 2024

Norwegian University of Science and Technology
Faculty of Natural Sciences
Department of Biology

NTNU
Norwegian University of
Science and Technology

Abstract

Temperatures are rising globally, with an amplified effect in the Arctic. This has caused sea-ice to melt, altering the habitat of organisms living there. In northern Baffin Bay tendencies towards a more stratified, hence more oligotrophic, surface and increased light availability are changing the fundamental criteria for diatom growth. As the base of the local food-web, a shift in primary production may affect the whole ecosystem. The goals of this study were to assess the composition and food-web dynamics of the protist community in northern Baffin Bay during the abnormally warm and ice free October of 2021. A novel video microscope, namely the Planktoscope, was further evaluated in assessment of these analyses.

Protist growth and grazing rates were assessed through a dilution experiment, by performing linear regression on microscopy counts. The same samples were analyzed by the Planktoscope to test its accuracy. The latter was not proven optimal for this experimental set-up. However, traditional light microscopy revealed a protist community dominated by small cells, with dinoflagellates being the most numerous taxa. Growth occurred amongst most diatoms with less to negative growth rates for most heterotrophic ciliates and dinoflagellates. Low grazer selectivity by heterotrophic protists and copepods were also observed. As a snapshot of recent conditions, these results provide a small piece of the large puzzle revealing the effects of climate change in Arctic ecosystems.

Key words: Arctic, Baffin Bay, climate change, protist, community, growth and grazing

Sammendrag

Globale temperaturer øker, med en forsterket effekt i Arktis. Dette har ført til at havis smelter, som igjen endrer habitatet til arktiske organismer. I den nordlige Baffinbukta ser man at en mer lagdelt, og dermed mer næringsfattig, overflate samt økt lystilgjengelighet endrer det fundamentale grunnlaget for diatomvekst. Som basen i det lokale næringsnettet, kan et potensielt skifte i primærproduksjon påvirke hele økosystemet. Dette studiet hadde som mål å undersøke samfunnssammensetning og trofisk dynamikk blant protister i den nordlige Baffinbukta under en unormalt varm og isfri oktober-måned, som fant sted i 2021. Et nyutviklet videomikroskop, kalt Planktoscope, ble også evaluert i å utføre disse analysene.

Vekst og beiterater for protister ble vurdert gjennom et fortynningseksperiment, ved å uføre lineær regresjon på antall individer av ulike grupper telt i mikroskop. Planktoscopets nøyaktighet ble så testet gjennom at det analyserte de samme prøvene og viste seg å ikke være tilstrekkelig i denne typen eksperiment. Lysmikroskopi kunne derimot avsløre et protistsamfunn dominert av små celler, og da særlig dinoflagellater. De fleste diatomgruppene viste seg å vokse, med lavere til negative vekstrater blant heterotrofe ciliater og dinoflagellater. Det ble også observert lite selektivitet blant beitende protister og kopepoder. Disse resultatene kan, som et øyeblikksbilde av nylige forhold, bidra med en liten brikke i det store puslespillet som effekter av klimaendringer på arktiske økosystemer utgjør.

Nøkkelord: Arktis, Baffinbukta, klimaendringer, protist, samfunn, vekst og beite

Acknowledgements

The data presented herein were collected by the Canadian research icebreaker CCGS Amundsen and made available by the Amundsen Science program, which is supported by the Canada Foundation for Innovation Major Science Initiatives Fund. The views expressed in this publication do not necessarily represent the views of Amundsen Science or that of its partners.

I would like to express my gratitude to the collaborative efforts of The Norwegian University of Science and Technology, University of Tromsø and Université Laval, whose support made the collection of the samples for this project possible. I would also like to extent special appreciation to my supervisors Maja Hatlebakk, Glaucia Fragoso and Geir Johnsen for the guidance and insightful feedback on this project. In particular, thank you to Maja Hatlebakk for your dedication, encouragement and valuable perspectives. Your contribution has been essential for me in this project and is much appreciated.

On a more personal note, thank you to my dear friends in Trondheim for all the support you provide me. Kristin Johnsen, thank you for always cheering me up and believing in me. Birgitte Amundsen, I have really appreciated your company and our adventures during our studies – from the Equator to the Arctic. To the girls at TBS, I could not have done it without you! I would also like to thank my family for inspiring me and encouraging me in reaching my goals.

May 2024, Trondheim
Ingeborg Skaar Dale

Table of content

List of figures

List of tables

Abbreviations

CO_2	Carbon dioxide
DE110, DE310, DE410	Sampling stations
CIII, CIV, CV	Copepodite stage 3, 4 and 5 of *C. glacialis*
BBSW	Baffin Bay Surface Water
ABPW	Arctic Basin Polar Water
WGCAIW	West Greenland Current Atlantic Intermediate Water
PSU	Practical Salinity Unit
Start, 20%, 100%, Cop	Treatments in the dilution experiment

1 Introduction

1.1 Climate change in the Arctic

Wide-ranging evidence shows that temperatures are rising globally due to a reinforcement of the greenhouse effect – caused by anthropogenic emissions of CO_2 and other greenhouse gasses (Manabe & Wetherald, 1975; Ramanathan *et al.*, 1985). Due to the high specific heat capacity of water, the oceans absorb and retain large portions of this heat and distribute it around the globe (Levitus *et al.*, 2000). The warming is further amplified in the Arctic due to atmospheric and oceanic heat flux convergence (Ting *et al.*, 2009; Yang *et al.*, 2010) in combination with other factors such as loss of insulating sea-ice (Serreze *et al.*, 2009), albedo feedback (Perovich *et al.*, 2007), increased cloud cover (Winton, 2006) and increasing concentrations of black carbon aerosols (Shindell & Faluvegi, 2009).

An area highly affected by arctic amplification is northern Baffin Bay, Canada. Here, a significant increase in oceanic temperatures has been seen over the past decades, mainly caused by the inflow of warmer North Atlantic water (Levitus *et al.*, 2000; Zweng & Münchow, 2006). This has led to earlier ice break-up and melting during spring and later ice formation during fall (Ballinger *et al.*, 2022; Onarheim *et al.*, 2018). Such an increase in the annual ice-free season may have large implications for both the local marine ecosystem and the Inuit communities depending on it (Cooley *et al.*, 2020; Meier *et al.*, 2006).

1.2 The planktonic community of northern Baffin Bay

A fundamental, ecological consequence of reduced sea-ice extent in the Arctic is the changes it causes to phytoplankton productivity (Ardyna & Arrigo, 2020). While a longer phytoplankton growing season with increased pelagic primary production is seen in most Arctic waters (Arrigo *et al.*, 2008), phytoplankton biomass and production has been observed to decrease in northern Baffin Bay during recent years. This decrease has been linked to altered seasonal progression and sea-ice dynamics with their respective effects on vertical stratification and freshwater input (Blais *et al.*, 2017).

Historically, northern Baffin Bay has been characterized as a well-mixed, nutrient rich, eutrophic system based on larger diatoms(Aksu & Piper, 1979; Tremblay *et al.*, 2006). The area has extensive periods of primary production lasting up to 6 months, with mainly two diatom genera dominating: *Thalassiosira* spp. and *Chaetoceros* spp. The prior has been observed to have an intense but transient bloom in May followed by a bloom of the latter between June and September (Booth *et al.*, 2002). Other phytoplankton species present during growth season include diatoms such as *Cylindrotheca closterium*, *Leptocylindrus* spp. and *Rhizosolenia* spp. in addition to autotrophic dinoflagellates (Lovejoy *et al.*, 2002).

The diatoms of northern Baffin Bay play an important role in the ecosystem of the area serving as a base of the food web. Some of their produced biomass sinks out of the euphotic zone as marine snow, with a small portion reaching the benthos. However, most of the biomass is consumed by pelagic consumers, with the majority of grazing occurring in the euphotic zone (Tremblay *et al.*, 2006).

Major grazers of diatoms in this region are microzooplankton and mesozooplankton. Microzooplankton in this area mainly constitutes heterotrophic alveolates, which has been seen to dominate in the post bloom plankton community during fall. Dinoflagellate genera observed in northern Baffin Bay include *Amphidinium* spp., *Gymnodinium* spp., *Gyrodinium* spp., *Protoperidinium* spp. and *Torodinium* spp. (Lovejoy *et al.*, 2002). While the dominating ciliates in the area mainly comprises the oligotrich species of *Lohmaniella* spp., *Strombidium* spp. and *Laboea* spp. (Paranjape, 1987; Tremblay *et al.*, 2006). In addition to being important grazers of phytoplankton, microzooplankton also take part in recycling of nutrients through excretory activity (Harrison, 1980).

The dominant species of mesozooplankton present in northern Baffin Bay, in terms of biomass, are the copepod species of *Calanus hyperboreus*, *Calanus glacialis* and *Metridia longa* (Stevens *et al.*, 2004). All three species have been found to feed omnivorously to various degrees, with *C. hyperboreus* being primarily herbivorous, *C. glacialis* omnivorous dominated by herbivory and *M. longa* omnivorous dominated by carnivory (Hobson *et al.*, 2002). The diets of these copepods mainly consist of diatoms, microzooplankton and microbial material with relative contribution varying with availability (Stevens *et al.*, 2004). Earlier findings for instance indicate that the degree of omnivory in these species is inversely related to diatom availability (Stevens *et al.*, 2004; Tremblay *et al.*, 2006). Furthermore, the arctic copepods are found to be the key link between primary producers and higher trophic levels (Falk-Petersen *et al.*, 2007). They are thus supporting the rich fauna of birds and marine mammals, present in the area (Hobson *et al.*, 2002; Holst *et al.*, 2001; Karnovsky & Hunt, 2002).

In other words, northern Baffin Bay poses a productive, intricate ecosystem with multiple interconnected parts – highly dependent on their planktonic base. Unfortunately, the balance of this base is expected to be vulnerable to projected changes in stability of the water column in regard to temperature, stratification and nutrient availability (Steinacher *et al.*, 2010). A potential imbalance can further change the carbon flow to higher trophic levels and the capacity of the Arctic Ocean to act as a CO_2 pump (Kirchman *et al.*, 2009). Effects on the global carbon cycle may also be amplified by a predicted increase in plankton respiration, that has been observed during warmer springs and summers in other Arctic regions (Vaquer-Sunyer *et al.*, 2010). These findings emphasize the importance of studying plankton in relation to climate change.

1.3 Studying plankton

Plankton are notably good indicators of environmental change due to their short generation time and rapid distributional responses to altered water circulation and condition (Hays *et al.*, 2005; Taylor *et al.*, 2002). Despite their importance, this group is generally understudied (Garcia *et al.*, 2022).

Ever since the 1800s, taxonomic analyses of plankton samples have remained labor intensive. Assessment of water samples through traditional microscopy often involves quantifying and sorting large amounts of individuals into taxonomic groups – giving a high sample processing time. This leads to a substantial delay in analyses and interpretation of data after sampling efforts (Benfield *et al.*, 2007). In addition, processing of plankton samples requires a specialist able to distinguish subtle differences in morphology. Attempts to accelerate the processing time can further cause fatigue

leading to a risk of higher error rates (Culverhouse *et al.*, 2003). In other words, new methods to accelerate processing of plankton samples, while still ensuring accuracy, are desired.

Video microscopy is a promising way of optimizing traditional methods. In this approach, samples are ran through a flow-cell where a camera records their content – magnified by lenses (Davis *et al.*, 1996). By providing images, this method gives a permanent record of sample content and an option for random subsampling. Additionally, having images as output opens a possibility for pattern recognition and machine learning, which drastically increases efficiency and decreases cost of sample analyses (Benfield *et al.*, 2007). However, the challenges of providing such algorithms are numerous. Not only are plankton a considerably heterogenic group with large differences in size and morphology (Sournia, 1982), they also live in a medium containing multiple non-living targets such as detritus and fecal pellets (Orenstein *et al.*, 2022). Practical obstacles such as orientation of the plankton in relation to the camera and clustering of individuals also pose some challenges in detection (Luo *et al.*, 2018). But, if successfully executed, video microscopy combined with artificial intelligence will provide unparalleled insight to the ecology of marine plankton (Benfield *et al.*, 2007).

An example of a novel and accessible video microscopy device is the Planktoscope. This is a high-throughput instrument autonomously providing images of water samples, that can be used in quantification and identification of plankton (Mériguet *et al.*, 2022). The device is provided with a Raspberry Pi computer that can be controlled through Wi-Fi, and its software is based on preexisting programs such as Node-RED, for graphical user interface, and MorphoCut for segmenting images. The processed output can further be exported to an EcoTaxa server for taxonomic identification using machine learning. The Planktoscope is efficient, easy to use, lightweight and of low cost compared to other microscopes. It may therefore have potential for consistent, long-term measurements of plankton diversity if proven accurate (Pollina *et al.*, 2022).

1.4 Research aims

Finding more efficient ways to assess plankton communities, while ensuring accuracy, is of high interest – especially with the world oceans being subject to critical environmental changes. This will facilitate research on plankton communities in particularly vulnerable areas such as northern Baffin Bay. Until now, few studies have been conducted in this remote area of the high Canadian Arctic – especially considering the rapid changes it is subject to. An area previously known for its high productivity may now be shifting towards more oligotroph conditions as meltwater input enhances stratification of the surface (Ardyna *et al.*, 2011).

In this study, growth and grazing rates of protists in northern Baffin Bay were assessed through a dilution experiment during an exceptionally warm fall of late ice formation (figure 1)(The Copernicus Programme, 2021). Data for the estimated rates were obtained through measurements of chlorophyll *a* concentrations and microscopy counts of plankton in water samples. The latter was also used to get an overview of the protist community composition at the time. The assessed community dynamics were further looked at in relation to environmental parameters and compared to previous circumstances as described by the literature. The novel automated Planktoscope was

evaluated in these analyses by comparing its output with counts attained by traditional microscopy.

Summarized, this research therefore aimed to:

1. Compare the protist community composition of a year with late ice formation to earlier descriptions during regular conditions
2. Compare protist growth and grazing dynamics of a year with late ice formation with earlier descriptions during regular conditions
3. Verify the novel Planktoscope in assessment of plankton communities

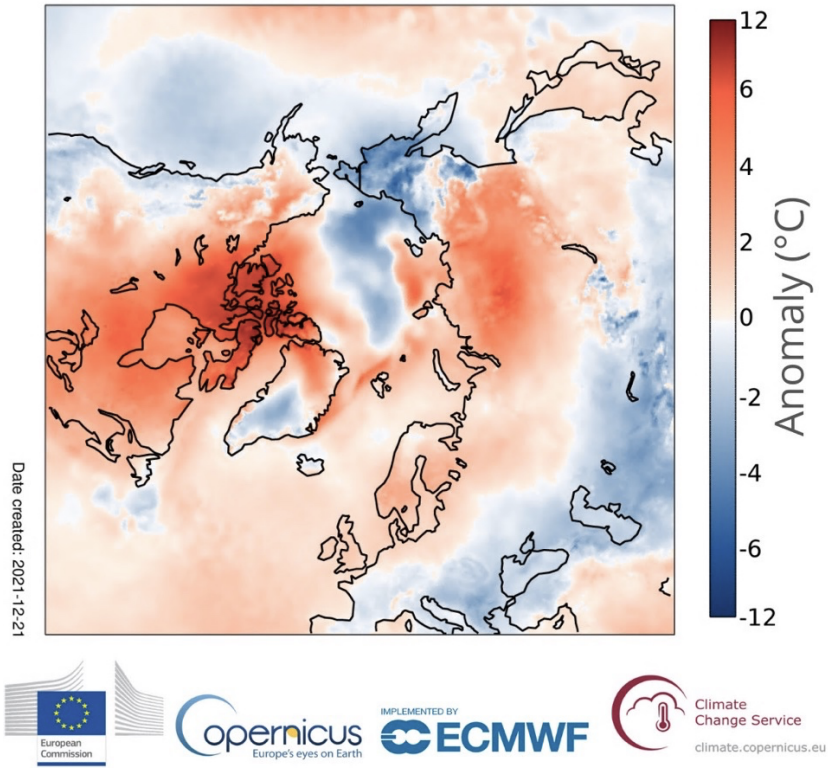

Figure 1: Arctic temperature anomalies of October 2021. The anomalies were based on temperature averages from 1991-2020. Exceptionally warm temperatures were seen for Nunavut, where norther Baffin Bay is located. Credit: modified from Copernicus Climate Change Service

2 Materials and methods

2.1 Sampling

The samples for this project were collected in Baffin Bay – a mediterranean sea connected to the Arctic and Atlantic Ocean through restrictive straits. The bay comprises a large abyssal plane located between the Baffin Island- and the Greenland continental shelf and is approximately 1400m long and 550m wide (figure 2) (Tang *et al.*, 2004).

Its northern parts, where sampling took place, are characterized by the inflow of cold, fresh, Arctic water through the Jones Sound, Barrow Strait and Nares Strait (Tang *et al.*, 2004). They are also subject to warmer, more saline, Atlantic water from the West Greenland Current, located below (Münchow *et al.*, 2015). Surrounded by ice-covered landmasses, the area receives a significant input of glacial meltwater and runoff during melting season, which further affects its stratigraphy (Addison & Bourke, 1987).

Moreover, northern Baffin Bay is partially covered by sea-ice most of the year with ice forming between September and November and melting between March and May (Ballinger *et al.*, 2022). Polynyas occur in the area, during winter and early spring, due to the combined effects of ice divergence and forced convection of warm water (Steffen, 1985). The light climate at this latitude is seasonally alternating between polar night and midnight sun.

This sets the stage for sample collection, which occurred during post-bloom conditions in October 2021 on the Dark Edge research cruise. The expedition was conducted by CCGS Amundsen – a Pierre Radisson-class icebreaker operated by the Canadian Coast Guard. Three different sample stations were chosen: DE110, DE310 and DE410, where a Niskin rosette collected water samples at approximately 30m depth (figure 2)(table 1). Attached was a Seabird CTD, measuring salinity, temperature, depth and chlorophyll *a* concentrations.

Figure 2: Map over sampling area and stations. DE110 is located in the northwestern part of Baffin Bay, DE310 in the southern Smith Sound and DE410 in the Jones Sound. Created with Google My Maps. Modified using Canva.com.

Table 1: Time, position and depth of sampling. Samples were taken between the 13th and 15th of October at 30 m depth.

Station	Date	Latitude	Longitude	Bottom depth(m)	Sampling depth(m)
DE110	13.10.21	76.0345773 °N	-077.2452833 °W	300	30
DE310	17.10.21	78.1697367 °N	-074.4030672 °W	700	30
DE410	20.10.21	75.9598238 °N	-085.5853352 °W	600	30

2.2 Dilution experiments

Following collection, the water samples were screened over 180μm mesh to exclude mesozooplankton grazers. Then growth and grazing experiments were conducted using the dilution method (Landry *et al.*, 1995; Landry & Hassett, 1982) with a two-point modification (Landry *et al.*, 1984; Lawrence & Menden-Deuer, 2012). By providing two levels of dilution, thus two levels of grazing pressure, and by looking at protist abundances before and after an incubation period, rates of growth and grazing were assessed. For further detail on the assumptions of this experiment see section 2.5.

Initially, six start samples of pre-screened seawater were fixated in triplicates of acidic Lugol's iodine solution (1.0 % final concentration) and neutral Lugol's iodine solution (0.5 % final concentration). Two fixatives with different conservational properties were utilized in case of degradation of material. The prior is better at preserving silicate shells of diatoms while the latter better sustaining calcareous flagellates (Anderson & Karlson, 2017). Remaining of the collected seawater was then also arranged in triplicates before undergoing three different treatments in 2L transparent plastic bottles (figure 3).

The first triplicate was diluted to 20% by adding seawater pre-filtered with a Whatman GF/F glass fiber filter (<0.7 μm pore size) collected from the sampling site at corresponding depth. The second and third triplicate remained at 100% concentration. Furthermore, copepods of the species *Calanus glacialis*, mainly stage CIV but occasionally CIII and CV, were added to the third triplicate to assess grazing rates when including a third trophic level. The experiment ran for 48-65 hours in incubation chambers on deck – simulating *in situ* temperature and ambient light conditions. Natural movement from the ship prevented plankton from settling.

After incubation, two samples were taken from each triplicate of each treatment and transferred to brown glass bottles, giving a total of 24 samples from each station. Concentrations of chlorophyll *a* was measured in all samples, as an indication of autotrophic plankton biomass, using fluorometry. Nitrate, nitrite, phosphate, silicate and ammonium were measured by an autoanalyzer. Half of the samples were then fixated in acidic Lugol's solution and half in neutral Lugol's solution to the same concentrations as the start samples. Two replicates of the samples preserved in acidic Lugol's solution for each treatment at each station were further examined. However, an exception was made for the diluted treatment at station DE310, due to loss of materials, where samples fixated in neutral Lugol's solution were used instead.

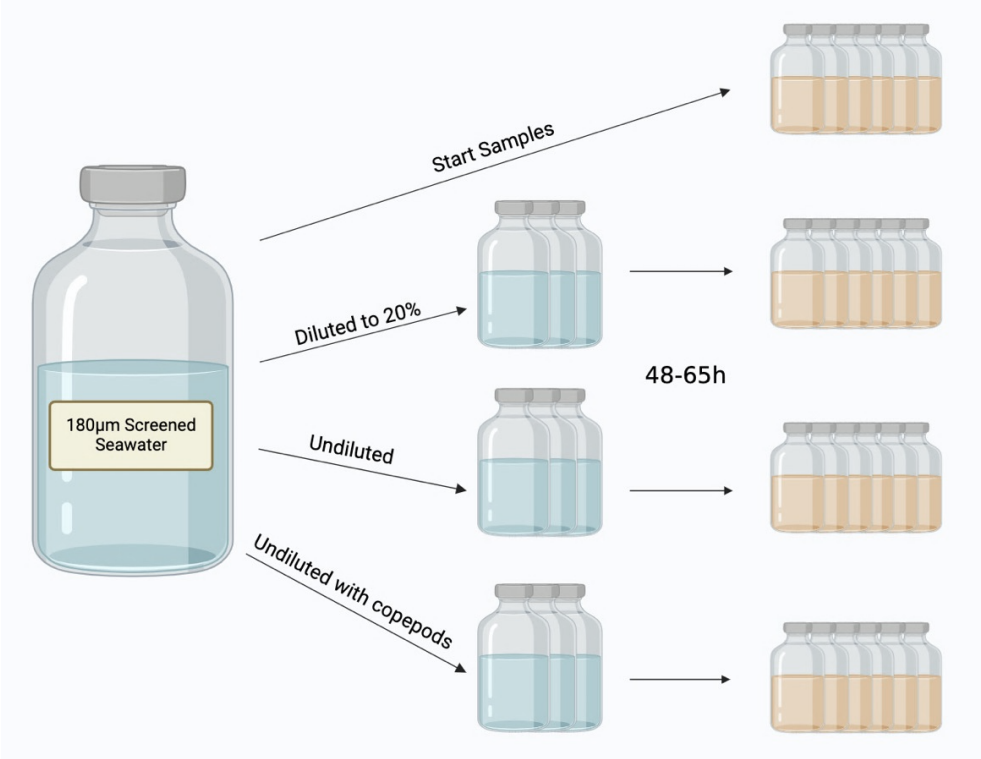

Figure 3: Experimental set-up of the *in vivo* dilution experiments. Start samples were provided as a basis of *in situ* conditions. Two levels of concentration (20% and 100% of start samples) were used to assess grazing rates over the incubation period of 48-65 hours. Growth was also estimated from start to end. Copepods were further added to one treatment to determine how this third trophic level affected grazing rates. Samples were fixated after the experiment. Figure created with BioRender.com

2.3 Microscopy counts

Analyses of the samples were conducted using the Utermöhl technique (Utermöhl, 1958). The preserved seawater was carefully mixed by rotation, transferred to 100mL cylinders and left for settling onto a slide with a small cavity for 48 hours (figure 4). Vacuum was created by adding water droplets to the interface between cylinder and slide and by pushing excess sample liquid off with the glass lid of the chamber. Where samples contained less than 100mL, seawater filtered through 0.2µm mesh was added to make sure the chambers were properly sealed. The added seawater was noted and later accounted for.

When the plankton were fully settled, the cylinder was carefully replaced by a cover glass for light microscopy. Vacuum was maintained by pipetting water in the interface between slide and cover. Remaining of the sample was then discarded into a tray below and transferred to a squeeze bottle. The following analyses were conducted by inverted microscopy using a Leica DM IRB.

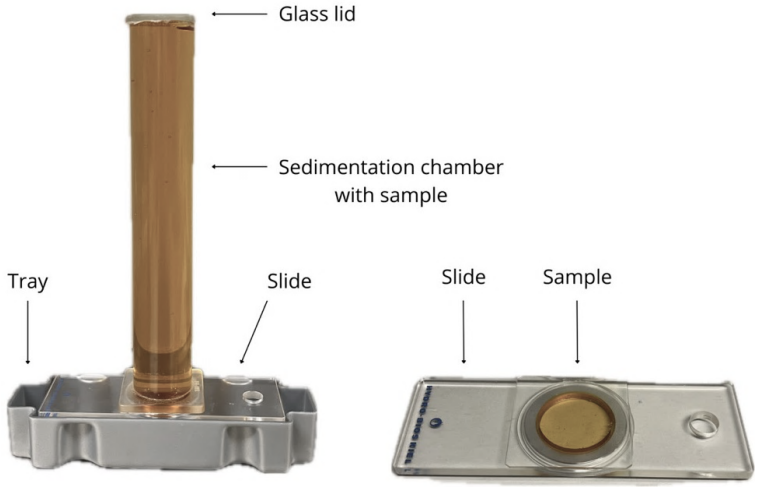

Figure 4: Components of the Utermöhl sedimentation technique. Samples were poured into the sedimentation chamber where its content settled on a slide. The slide was then analyzed with microscopy. Remaining of the sample was discarded into the tray below. Created in Canva.com.

Microscopy counts were attained by visually scanning the slides in vertical lines on a magnification of 200x. All detected protists were then assigned groups based on taxonomy and size (table 2). For samples of low cell density, the whole area of the slide was examined. However, when cell densities were high, a smaller fraction of the area was counted assuring at least 100 specimens of the most abundant species and 300 specimens in total (average of 554 cells per sample). Images were also taken along with scanning, using the ZEISS ZEN core software (version ZEN 2 core SP1). Ultimately, the counts were noted in an Excel worksheet for further data handling. All the equipment was properly rinsed in tap water, followed by distilled water, between samples to avoid contamination.

Table 2: Overview of defined groups based on taxonomy and size.

Major groups
Diatom <20μm
Diatom 20-50μm
Diatom >50μm
Dinoflagellate <20μm
Dinoflagellate 20-50μm
Dinoflagellate >50μm
Ciliate <20μm
Ciliate 20-50μm
Ciliate >50μm

2.4 Planktoscope

After microscopy counting, the samples were poured from the slide-chamber into centrifuge tubes. Small amounts of the remaining Lugol's solution in the squeeze bottle were used to rinse, collecting plankton adhering to the glass. The tubes were then stored in a dark cabinet, due to the light sensitive nature of the preservative, until further processing for the Planktoscope (figure 5).

Two levels of sample concentration were tested in the Planktoscope. Initially, the samples were standardized to 5 mL by removing excess Lugol's solution with a 5μm filter attached to a pipette – ensuring that specimens >5μm remained. Later, samples were concentrated further down to 0.5 mL to increase detection of plankton by the camera system. After each step of concentration, samples were transferred to the Planktoscope where adjustments to settings were made.

Primarily, the optical set-up of the Planktoscope was configurated by adjusting light and focus on the flow-cell (μ-Slide I Luer, 0.2 mm) to ensure clear plankton images (2.8

μm/px, 1920 x 1018px frame). Lenses (M12) of different focal lengths were also tested to optimize visualization. Information about the samples was then plotted into the system including sample-ID, coordinates and volume in addition to applied sampling gear. For the first level of concentration multiple flow and acquisition rates were tested to find a feasible coverage of the sample while also avoiding settlement of plankton. When samples were more concentrated the device was set to acquire 100 images, pumping 0.005 mL through the flow-cell between each depiction, ensuring that the whole sample was recorded.

Following acquisition, the images were segmented by the Planktoscope and saved as a zip file, accessed through the cross-platform FTP application Filezilla. The file was then exported to EcoTaxa – a software application used for taxonomic annotation of plankton images, operated by Sorbonne Université and CNRS, France. In this software, segmented images were classified by machine learning algorithms giving taxonomic composition of the samples as output. The device was prepared for the next sample by pumping distilled water through the system multiple times, rinsing out remaining plankton and detritus.

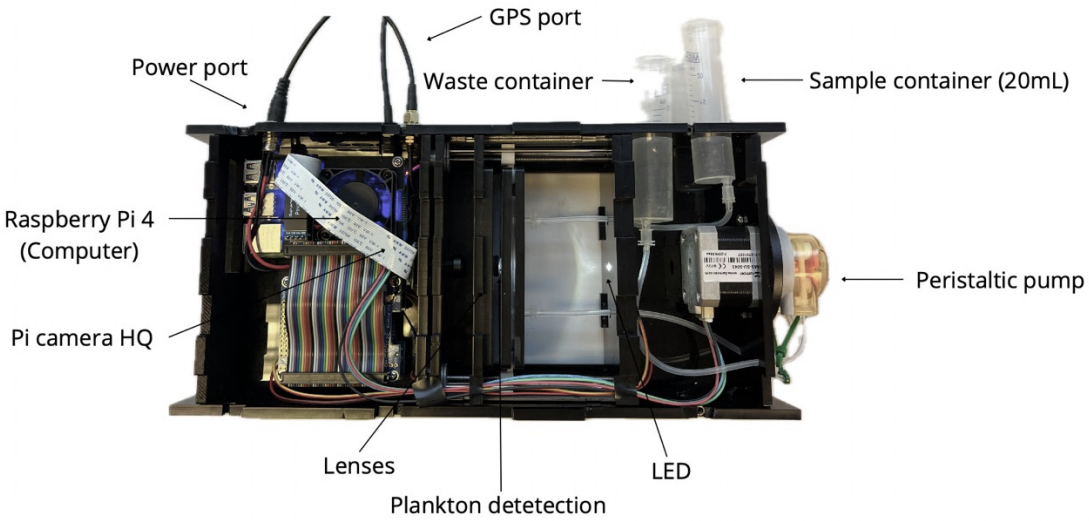

Figure 5: Planktoscope set-up. Samples were poured into the sample container and pumped through a flow-cell where a camera recorded its magnified content. The samples were then discarded into the waste container. Images taken were further segmented and analyzed.

2.5 Estimations of growth and grazing

Growth and grazing rates were assessed following the dilution approach introduced by Landry & Hassett (1982) as described in section 2.2. The method is based on the assumption that phytoplankton growth rates are independent of the effect of dilution on population density. Additionally, it assumes that the rate of phytoplankton mortality due to microzooplankton grazing is proportional to the dilution effect on grazer abundance. This can be applied to an exponential model of population growth (1), making it possible to calculate net rate of change (k_d) based on initial (P_0) and final parameters (P_t) where t is the duration of the experiment in days:

$$k_d = \frac{1}{t} \ln \left(\frac{P_t}{P_0}\right) \quad (1)$$

In this case, the formula was applied to initial and final measurements of chlorophyll *a* concentrations as measured by fluorometry and of microscopy counts of the defined groups (table 2).

Estimates of growth and grazing rates were then performed through a two point regression (α=0.05) as detailed by Chen (2015). In this case plankton net growth rate (k_d) was the response variable and the fraction of undiluted seawater was the predictor (here 0.2 and 1). The intercept of this regression corresponds to the plankton instantaneous growth rate (μ)(3) while the instantaneous grazing rate is given by the regression slope (m)(2).

Assuming a linear relationship, instantaneous grazing rates (m) per day can be estimated by taking the dilution factor (D) into account as following:

$$m = \frac{\bar{k}_{0.2} - \bar{k}_1}{D} \quad (2)$$

Instantaneous growth rates (μ) per day can then be estimated as following:

$$\mu = \bar{k}_1 + m \quad (3)$$

A more intuitive way of presenting growth rates is by considering cell divisions per day (λ)(4), given by:

$$\lambda = \frac{\mu}{\ln(2)} \quad (4)$$

For this project, estimated growth rates and their respective standard errors are therefore converted to, and presented as, cell divisions per day.

Traditionally, dilution experiments have been conducted to estimate growth and grazing rates of phytoplankton and not heterotrophic ciliates and dinoflagellates. Yet, these groups meet the assumptions of this approach to some degree. Both ciliates and dinoflagellates have for instance been found to persist regardless of low phytoplankton abundances, and are thus likely to be moderately affected by dilution and less prey encounters over this short incubation period (Franzé & Modigh, 2013; Sherr & Sherr, 2007). The protists are also found to graze on each other and are important prey of copepods such as *C. glacialis* (Franzé & Modigh, 2013; Levinsen & Nielsen, 2002; Sherr & Sherr, 2007). Hence, the estimated rates of growth and grazing of these groups are indicative of *in situ* trends and are therefore presented in this thesis.

2.6 Statistical analyses and data presentation

All statistical analyses and plots for this project were conducted using the software programming language R (version 4.2.3) through RStudio™ (version 2023.06.2). Modifications to plots were further made in Canva.com to increase readability. Abundance data was graphically presented in Microsoft© Excel for Mac (version 16.66.1).

Regarding statistics, average nutrient concentrations and chlorophyll *a* measurements were compared through a two-way ANOVA. This enabled evaluating differences between stations and revealed progression in samples throughout the experiment. Growth and grazing rates were further assessed through linear regression. Both average nutrient concentrations and estimated growth and grazing rates are stated as parameter estimates ± standard errors. They are further presented in tables made in Microsoft© Word for Mac (version 16.66.1).

3 Results

3.1 Environmental conditions

Analyses of environmental parameters indicate the presence of three distinct water masses in the sampling area – all of Arctic and Atlantic origin (Muench, 1971)(figure 6). Observations of a fresh surface layer, for instance, matches earlier descriptions of Baffin Bay Surface Water (BBSW) with a defined salinity <32.8 (Addison & Bourke, 1987; Coachman & Aagaard, 1974; Fissel *et al.*, 1982). Below was a layer of cold and slightly more saline water corresponding to previous descriptions of Arctic Basin Polar Water (ABPW) as defined with temperatures <0 °C and a salinity <34.8 (Addison & Bourke, 1987; Aagaard & Coachman, 1968). Towards the bottom, temperatures and salinities increased. These observations are in agreement with earlier descriptions of West Greenland Current Atlantic Intermediate Water (WGCAIW) with a defined salinity of 33.8 to 34.5 and temperatures >0 °C (Addison & Bourke, 1987; Aagaard & Coachman, 1968).

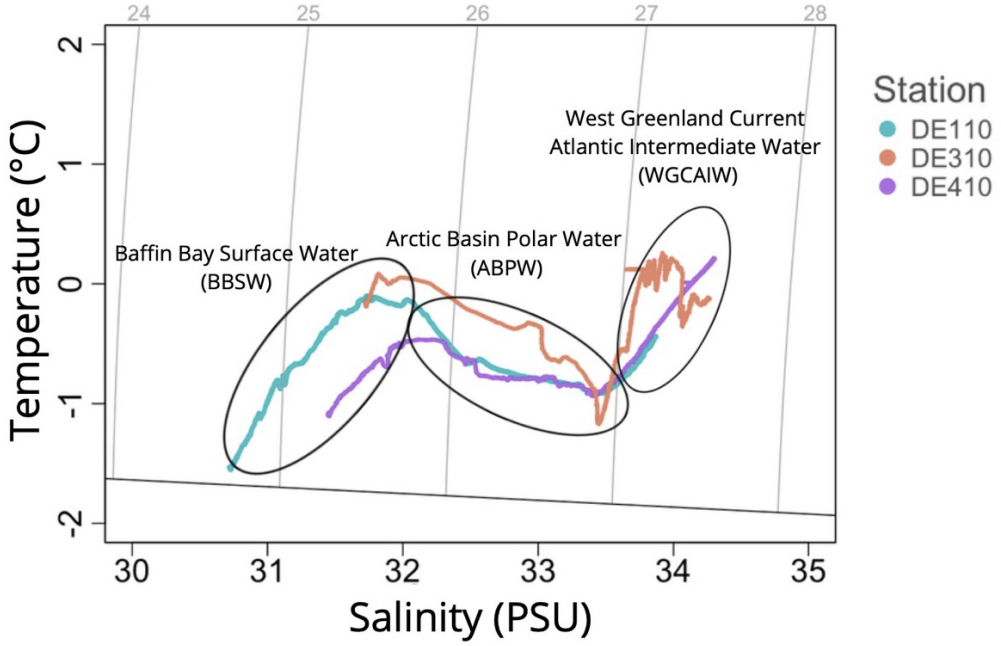

Figure 6: Temperature and salinity plots for sample stations. Three water masses were observed: Baffin Bay Surface Water(BBSW) at the top with Arctic Basin Polar Water(ABPW) below. An influence from the West Greenland Current Atlantic Intermediate Water (WGCAIW) was observed towards the bottom. Station DE110 is here marked in blue, DE310 in orange and DE410 in purple.

The presence of these water masses was also reflected in the vertical profiles of the stations (figure 7-9). At station DE110 the mixed layer (corresponding to BBSW) reached

down to around 30 m, where sampling was conducted (figure 7). This layer was found to have a temperature of around -1.5 °C and a salinity of around 30.8. Sampling was conducted in the euphotic zone with chlorophyll *a* concentrations of 0.22 to 0.25 μg/L.

Furthermore, the station had a depth of around 300 m, solely subzero temperatures, and salinities below 33.9, and is therefore likely to be dominated by ABPW (Here in the salinity range of 30.8 to 33.9 and a temperature range of -1.5 to -0.1 °C). However, a halocline and thermocline is seen towards the bottom, indicating some influence by WGCAIW.

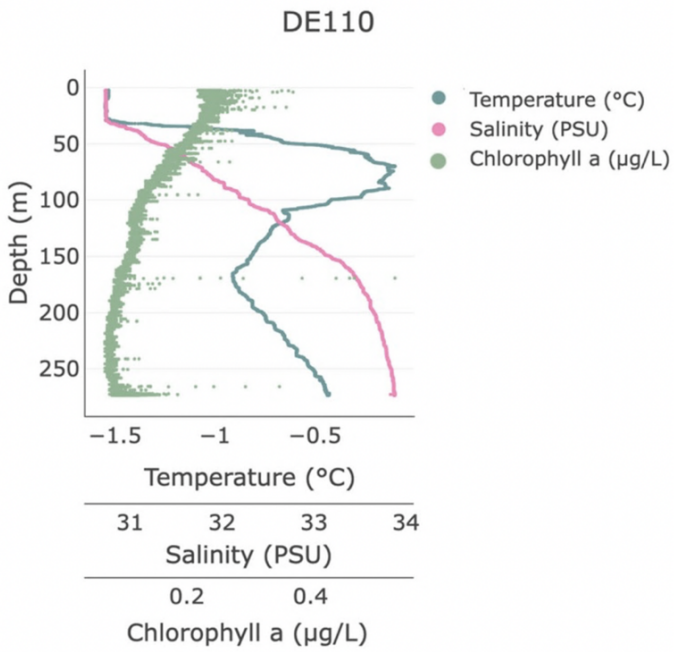

Figure 7: Vertical profile of station DE110. The figure shows how temperature, salinity and chlorophyll *a* changes with depth. A dominance of ABPW was seen at this station with a mixed layer of ~30m depth and some influence from WGCAIW towards the bottom.

Sampling at station DE310 also occurred in the mixed layer, which here reached down to around 35 m (figure 8). The temperature for this layer was around -0.2 °C and the salinity around 31.7 – both values higher compared to station DE110. Chlorophyll *a* concentrations here ranged between 0.26 and 0.32 μg/L at the sampling depth.

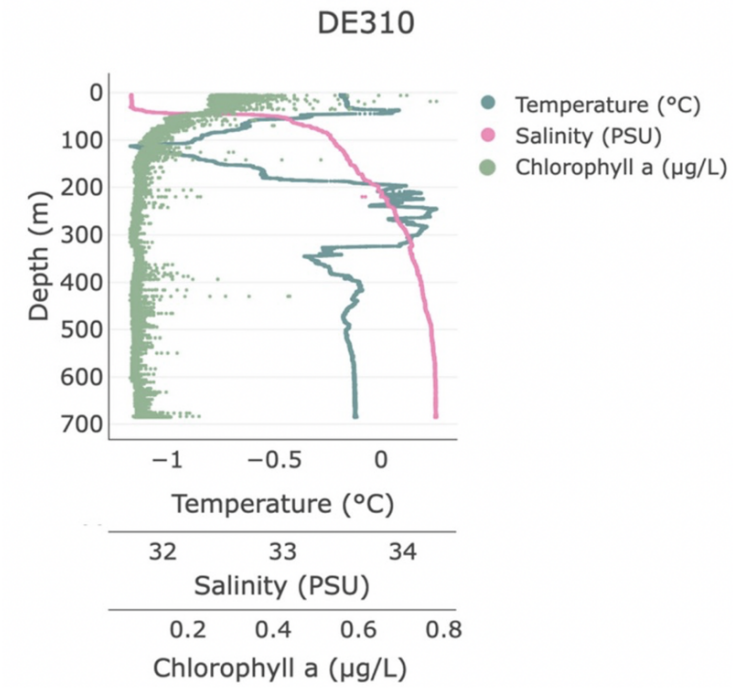

Figure 8: Vertical profile of station DE310. The figure shows how temperature, salinity and chlorophyll *a* changes with depth. A mixed layer was seen down to ~35 m, with ABPW between 35 to 200 m. An influence by WGCAIW was apparent below 200 m.

Below the mixed layer, a thermocline was observed, ending in a temperature minimum of -1.2 °C at 100 m depth – presumably caused by ABPW. With a salinity range of 31.8 to 33.7 and a temperature range of -1.2 and 0.1 °C, this water mass seemed to be present between 35 and 200 m at this station. Below, down to the bottom, WGCAIW was seen with salinities and temperatures of 33.7 to 34.3 and -0.3 to 0.3 °C, respectively.

At station DE410, the mixed layer appeared to be around 20 m deep with a temperature of -1.1°C and a salinity of 31.5 (figure 9). Beneath, temperatures stayed low until a rapid increase occured after ~250 m, marking a transition from ABPW to WGCAIW. The ABPW at this station had a salinity range of 34.1 to 34.3 and temperatures of -1.1 to 0 °C. WGCAIW had a salinity range of 34.1 to 34.3 and a temperature range of 0.0 to 0.2 °C.

In contrast to station DE110 and DE310, sampling at station DE410 was conducted below the mixed layer. Measurements at sampling depth showed a temperature of -0.8 °C and a salinity of 31.7. Concentrations of chlorophyll *a* were between 0.18 and 0.23 μg/L.

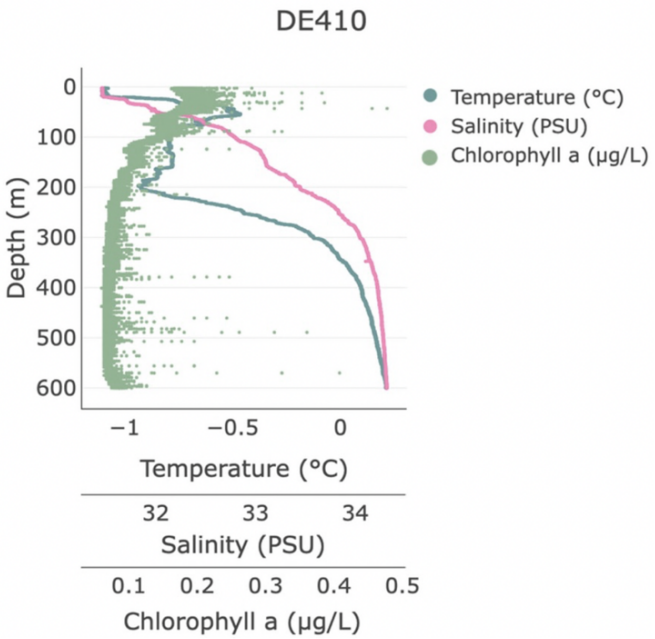

Figure 9: Vertical profile of station DE410. The figure shows how temperature, salinity and chlorophyll *a* changes with depth. This station had a mixed layer of ~25 m and ABPW down to around 250 m. Below, temperature and salinity increases indicating mixing with WGCAIW which is fully present below 350 m.

3.2 Nutrients

At the sampling depth of 30 m, all three stations had distinct nutrient compositions (table 3). Start samples at station DE110, representing *in situ* conditions, for instance revealed a nitrite concentration of 0.02 ± 0.00 μM and a nitrate concentration of 0.49± 0.02 μM. Concentrations of phosphate and silicate were measured to 0.50 ± 0.03 μM and 0.96 ± 0.00 μM, respectively, while ammonium had a concentration of 1.56 ± 0.08 μM.

Station DE310, however, had significantly higher concentrations of nitrite (0.09 ± 0.00, ANOVA, $p < 0.001$), nitrate (1.67 ± 0.02 μM, ANOVA, $p < 0.001$) and a silicate (1.62 ± 0.01 μM, ANOVA, $p < 0.001$), compared to station DE110. In contrast, concentrations of phosphate and ammonium were lower with concentrations of 0.37 ± 0.00 μM (ANOVA, $p < 0.001$) and 0.97 ± 0.07 μM (ANOVA, $p < 0.001$), respectively.

Station DE410 falls in the middle of station DE110 and DE310 for concentrations of nitrite (0.06 ± 0.00 μM, ANOVA, $p < 0.001$) and ammonium (1.05 ± 0.07 μM, ANOVA, $p < 0.001$). However, this station showed the highest values of nitrate with 2.13 ± 0.02 μM (ANOVA, $p < 0.001$) and silicate with 4.25 ± 0.01 μM (ANOVA, $p < 0.001$). Phosphate had a concentration of 0.49 ± 0.00 (ANOVA, $p = 0.984$).

Throughout the incubation period, nutrient concentrations varied to some extent for the different treatments. A comparison of start samples with incubated, undiluted samples indicate nutrient consumption and regeneration by the protist community. At station

DE110 nitrate and silicate was seen to significantly increase throughout incubation. Nitrate increased from 0.02 ± 0.00 to 0.03 ± 0.00 (ANOVA, $p = 0.001$) and silicate from 0.96 ± 0.00 to 1.73 ± 0.00 (ANOVA, $p < 0.001$). No significant change was found for nitrate and phosphate. Furthermore ammonium decreased from 1.56 ± 0.08 to 0.97 ± 0.08 (ANOVA, $p = 0.019$).

At station DE310 a significant increase in nitrate and silicate was seen. Nitrate increased from 1.67 ± 0.02 to 1.87 ± 0.02 (ANOVA, $p < 0.001$) and silicate from 1.62 ± 0.01 to 1.66 ± 0.01 (ANOVA, $p = 0.002$). No significant changes were seen for nitrite, phosphate and ammonium.

Furthermore, nitrate and silicate at station DE410 were shown to increase through incubation. Nitrate increased from 2.13 ± 0.02 to 2.92 ± 0.02 (ANOVA, $p < 0.001$) and silicate from 4.25 ± 0.01 to 4.70 ± 0.01 (ANOVA, $p = 0.002$). Nitrite, phosphate and ammonium had no significant changes.

Table 3: Average nutrient concentrations. Nitrite, nitrate, phosphate, silicate and ammonium concentrations were measured for start samples, diluted samples (20%), undiluted samples (100%) and undiluted samples with *C. glacialis* added (Cop) at each station.

Treatment	Nitrite (µM)	Nitrate (µM)	Phosphate (µM)	Silicate (µM)	Ammonium (µM)
DE110					
Start	0.02 ± 0.00	0.49 ± 0.02	0.50 ± 0.03	0.96 ± 0.00	1.56 ± 0.08
20%	0.04 ± 0.00	0.60 ± 0.02	0.48 ± 0.03	1.74 ± 0.00	1.06 ± 0.08
100%	0.03 ± 0.00	0.48 ± 0.02	0.52 ± 0.03	1.73 ± 0.00	1.21 ± 0.08
Cop	0.03 ± 0.00	0.47 ± 0.02	0.47 ± 0.03	1.74 ± 0.00	0.97 ± 0.08
DE310					
Start	0.09 ± 0.00	1.67 ± 0.02	0.37 ± 0.00	1.62 ± 0.01	0.97 ± 0.07
20%	0.10 ± 0.00	1.97 ± 0.02	0.37 ± 0.00	1.69 ± 0.01	1.23 ± 0.07
100%	0.09 ± 0.00	1.87 ± 0.02	0.36 ± 0.00	1.66 ± 0.01	0.85 ± 0.07
Cop	0.08 ± 0.00	1.86 ± 0.02	0.36 ± 0.00	1.66 ± 0.01	1.08 ± 0.07
DE410					
Start	0.06 ± 0.00	2.13 ± 0.02	0.49 ± 0.00	4.25 ± 0.01	1.05 ± 0.07
20%	0.05 ± 0.00	3.02 ± 0.02	0.63 ± 0.00	4.64 ± 0.01	1.37 ± 0.07
100%	0.05 ± 0.00	2.92 ± 0.02	0.63 ± 0.00	4.70 ± 0.01	0.95 ± 0.07
Cop	0.05 ± 0.00	3.28 ± 0.02	0.64 ± 0.00	4.80 ± 0.01	0.95 ± 0.07

3.3 Protist community composition

Taxonomic and dimensional composition of the protist community was analyzed in all samples through inverted microscopy. Start samples represented the *in situ* protist assemblage at the spatial and temporal point of sampling (figure 13).

The stations were generally dominated by dinoflagellates <20 µm ranging from 8.6 cells/mL at station DE410 to 15.7 cells/mL at DE110 (figure 13). Individuals of 20-50 µm were also noteworthy with the highest abundance of 2.6 cells/mL at station DE310. There were few individuals >50 µm present. Dinoflagellates were mostly seen in athecate forms including *Gyrodinium* spp., *Gymnodinium* spp. and *Amphidinium* spp., but thecate forms such as *Protoperidinium* spp. and *Phalacroma* spp. were also observed frequently (figure 10).

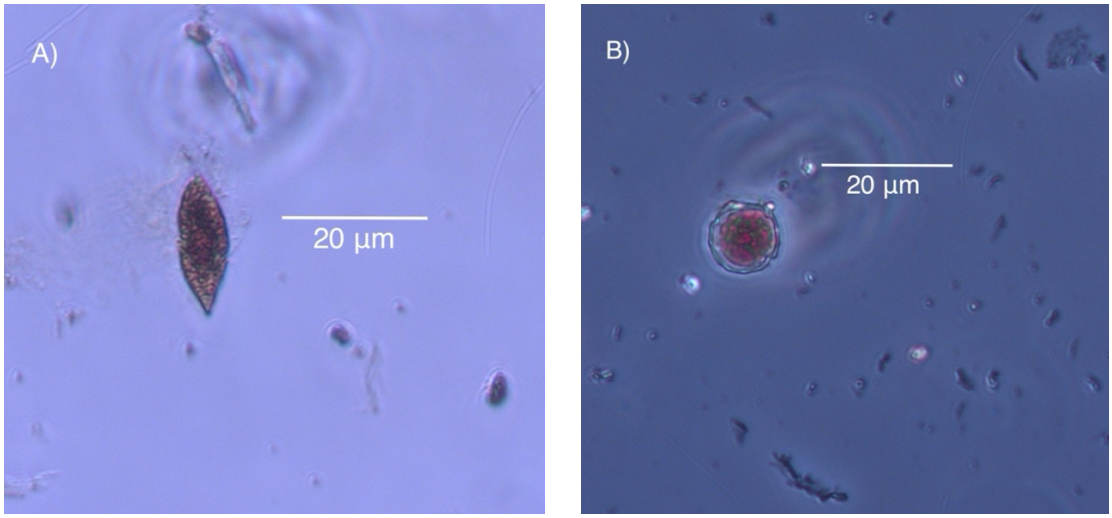

Figure 10: Light microscopy images of dinoflagellates. This taxa was mostly seen in athecate forms but some thecate forms also occurred. Images were taken at a magnification of 200 x. A) *Amphidinium* spp. – an athecate dinoflagellate. B) *Protoperidinium* spp. – a thecate dinoflagellate.

More variation was seen among stations in terms of diatoms. Where station DE110 and DE410 were numerically dominated by *Chaetoceros* spp., station DE310 was rich in chains of *Leptocylindrus* spp. (figure 11). These compositional differences were reflected in the dimensional abundance data (figure 13). Station DE110 and DE410 were for instance found to be richer in diatoms <20 µm (8.1 and 2.8 cells/mL respectively) while station DE310 contained more diatoms in the size class 20-50 µm (4.4 cells/mL). Individuals of other centric diatom genera were also observed at all stations including *Thalassiosira* spp., and *Rhizosolenia* spp. Some pennate diatoms also occurred, such as *Cylindrotheca closterium*. This was the most prevalent diatom >50 µm, accounting for the majority of diatoms in this group at all stations (0.2-0.4 cells/mL).

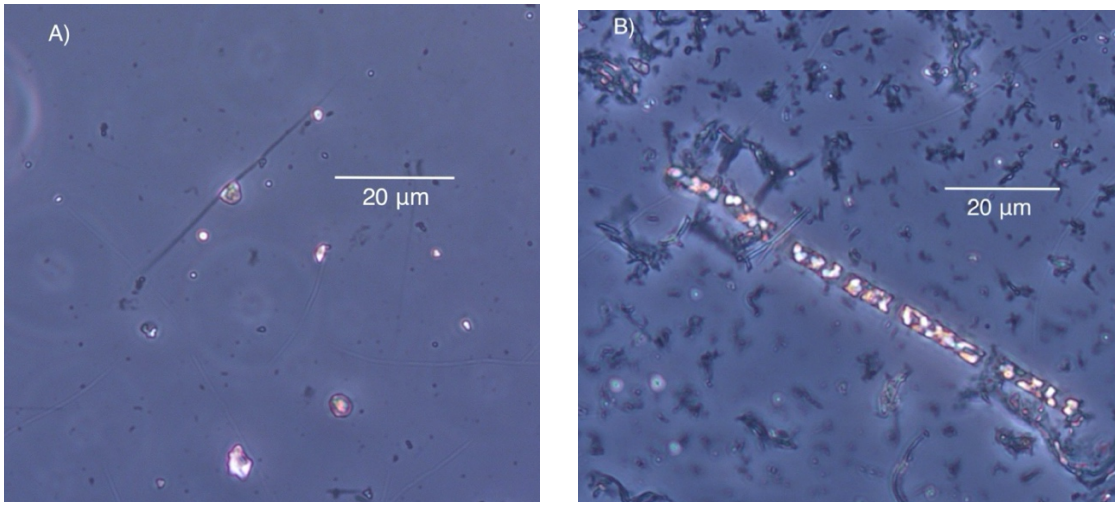

Figure 11: Light microscopy images of diatoms. Centric diatoms were more abundant, but pennate forms also occurred. Images were taken with a magnification of 200 x. A) *Chaetoceros* spp. – a centric diatom, dominating at station DE110 and DE410. B) *Leptocylindrus* spp. – a centric diatom dominating at station DE310.

Ciliates were less prevalent but still noteworthy in the samples. This taxon was mostly observed as individuals <20 µm with abundances between 0.6 cells/mL at station DE410 and 1.7 cells/mL at station DE310 (figure 13). A portion was also of sizes between 20

and 50 μm with abundances of 0.3 cells/mL at DE410, 0.7 cells/mL at DE110 and 0.8 cells/mL at DE310. The ciliates were exclusively of oligotrich forms with the dominant genera being *Strombidium* spp., *Laboea* spp., *Leegaardiella* spp. and *Lohmaniella* spp. (figure 12).

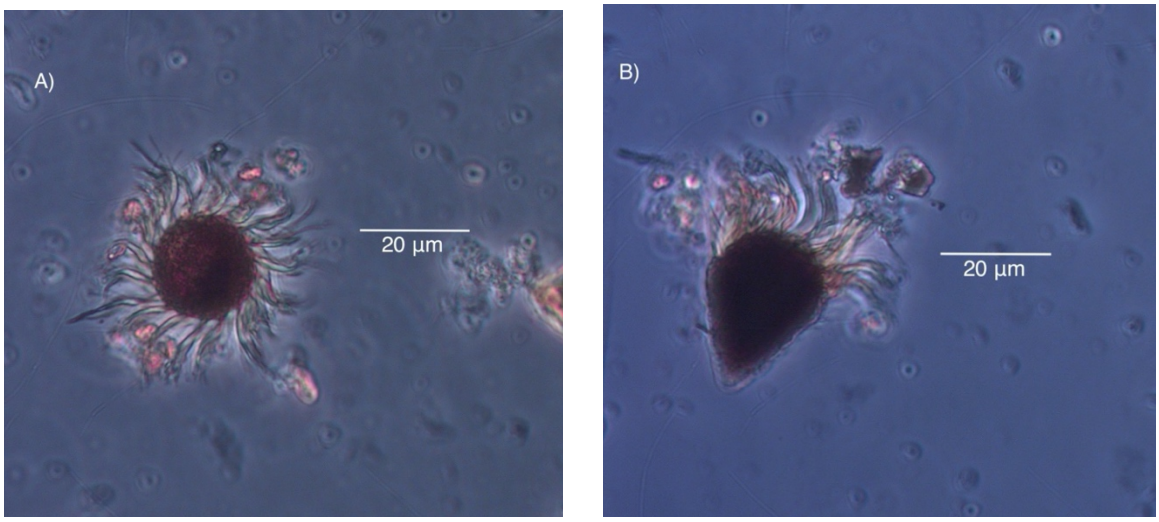

Figure 12: Light microscopy images of ciliates. These were exclusively in oligotrich forms. Images were taken with a magnification of 200 x. A) *Leegaardiella* spp.– an abundant oligotrich ciliate B) *Strombidium* spp. – another common oligotrich ciliate.

For most experimental groups, the initial abundances from the start samples decreased during incubation in both undiluted treatments at station DE110 and DE310. For station DE410 on the other hand, absolute abundances remained quite similar regardless of treatment at dilution factor 1 (figure 13).

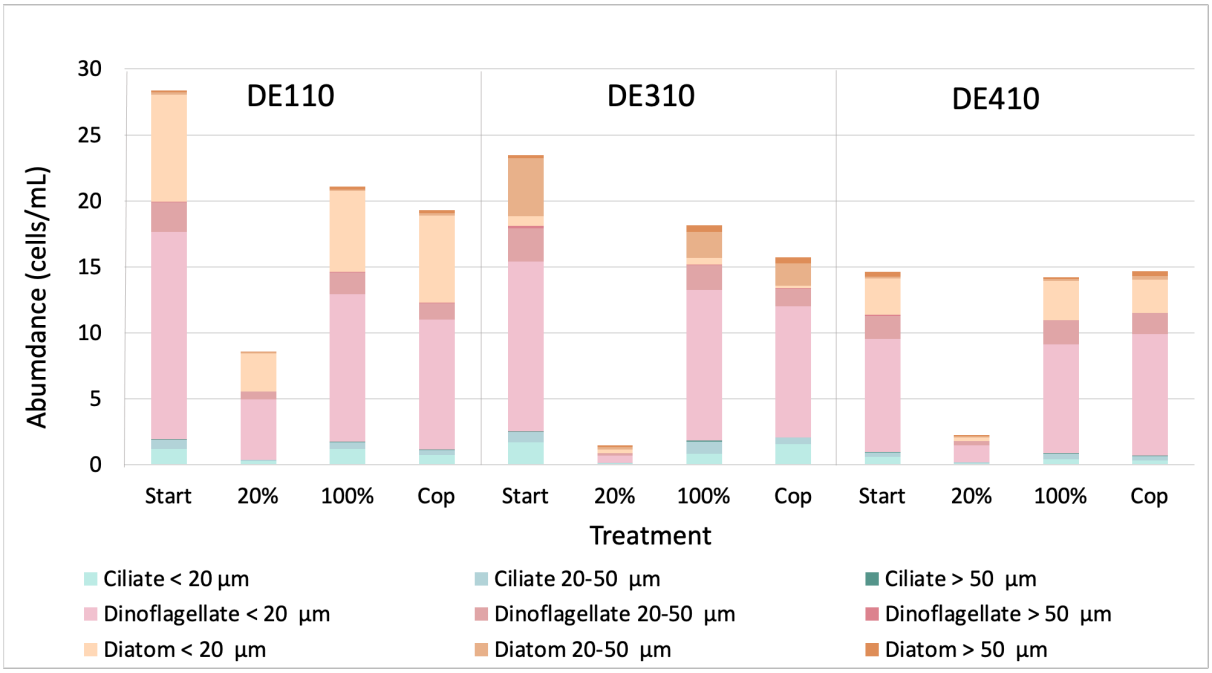

Figure 13: Average abundance of the experimental groups in samples. Ciliates, dinoflagellates and diatoms are marked in blue, pink and orange, respectively, with darker shades corresponding to larger size classes. Abundance is here measured in cells/mL and calculated for start samples, diluted samples (20%), undiluted samples (100%) and undiluted samples with *C. glacialis* added (Cop) at all three stations. Dinoflagellates dominated numerically at all stations, followed by diatoms and then ciliates. Small individuals were typically more numerous for all taxa.

3.4 Dilution experiments

Growth and grazing rates were estimated using data from both microscopy counts and measurements of chlorophyll *a* concentrations (figure 14). As also seen for *in vivo* chlorophyll *a* (figure 7-9), direct measurements in the start samples revealed a higher average concentration of 0.65 μg/L (ANOVA, p = 0.017) at station DE310 and a lower of 0.30 μg/L (ANOVA, p = 0.412) at station DE410. Measurements of chlorophyll *a* were also generally higher at station DE310 and lower at DE410 for the two undiluted treatments.

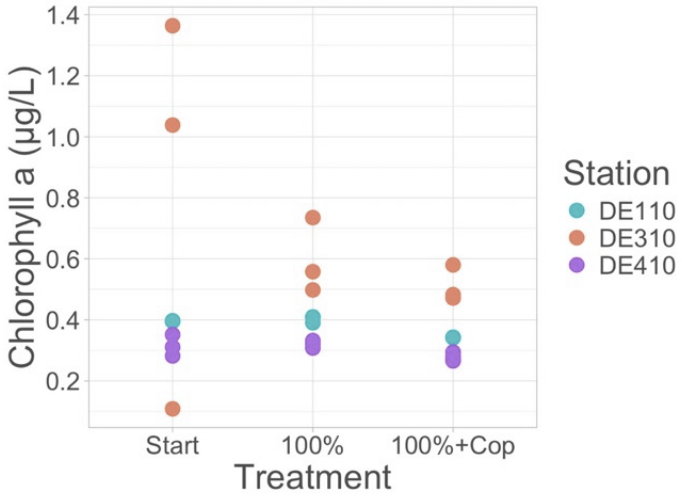

Figure 14: Chlorophyll *a* concentrations of samples. Station DE110 is marked in blue, DE310 in orange and DE410 in purple. These values were used in estimating growth and grazing rates of autotrophic plankton.

The growth rates estimated from chlorophyll *a* concentrations were positive for all three stations (table 4). The highest growth rate was seen at station DE410 (0.41 ± 0.07 cell div. d^{-1}, p = 0.003), followed by DE310 (0.20 ± 0.73 cell div. d^{-1}, p = 0.799). The lowest was seen at DE110 (0.11 ± 0.01 cell div. d^{-1}, p < 0.001).

In contrast, estimates of growth rates based on microscopy counts generally showed more growth at station DE110 for all taxa (table 4). Diatoms grew the most (0.42 ± 0.25 cell div. d^{-1} for <20 μm, 0.76 ± 0.40 cell div. d^{-1} for 20-50 μm and 0.14 ± 0.30 cell div. d^{-1} for >50 μm), followed by dinoflagellates (0.21 ± 0.30 and 0.26 ± 0.18 cell div. d^{-1} for groups <20 μm and of 20-50 μm, respectively). The lowest growth rates were seen amongst the ciliates with positive growth only seen in the group <20 μm (0.02 ± 0.30 cell div. d^{-1}).

Station DE310, on the other hand, showed the least growth. Negative growth rates were seen for the dinoflagellates <20 μm (-1.51 ± 0.54 cell div. d^{-1}) and of 20-50 μm (-1.20 ± 0.61 cell div. d^{-1}) as well as the ciliates <20 μm (-1.26 ± 0.69 cell div. d^{-1}) and of 20-50 μm (-1.46 ± 0.58 cell div. d^{-1}). The groups >50 μm, however, grew slightly (0.10 ± 0.65 cell div. d^{-1} for dinoflagellates and 0.27 ± 0.89 cell div. d^{-1} for ciliates). Positive growth rates were also seen in the diatoms <20 μm and >50 μm (0.47 ± 0.18 and 0.57 ± 0.31 cell div. d^{-1}, respectively), while the group of 20-50 μm had a negative growth rate (-1.11 ± 0.19 cell div. d^{-1}).

Little to no growth was seen for the ciliates (0.01 ± 0.20 and -0.29 ± 0.15 cell div. d^{-1} for <20 μm and 20-50 μm, respectively) and dinoflagellates (-0.26 ± 0.15 cell div. d^{-1} for <20 μm, -0.22 ± 0.33 cell div. d^{-1} for 20-50 μm and 0.23 ± 0.51 cell div. d^{-1} for >50 μm) of station DE410. Regarding diatoms, the higher growth rate was observed amongst individuals of 20-50 μm (1.72 ± 1.03 cell div. d^{-1}), followed by a slight growth of individuals >50 μm (0.23 ± 0.44 cell div. d^{-1}). Diatoms <20 μm showed a negative growth rate (-1.14 ± 0.71 cell div. d^{-1}).

Table 4: Growth rates of the experimental groups. Here measured in cell divisions per day over the course of 48-65 h. Positive and negative growth rates are marked in green and pink, respectively, with darker shades corresponding to higher rates. Where estimates were not available (NA), cells are marked in light grey. Growth were seen for most diatoms except those of 20-50 μm at station DE310 and <20 μm at station DE410. Negative growth rates were generally seen for ciliates and dinoflagellates, except for at station DE110 where positive rates were seen for most groups.

	Growth rates (cell div. d^{-1})		
Group	**DE110**	**DE310**	**DE410**
Ciliate <20 μm	0.02 ± 0.30	-1.26 ± 0.69	0.01 ± 0.20
Ciliate 20-50 μm	-0.21 ± 0.28	-1.46 ± 0.58	-0.29 ± 0.15
Ciliate >50 μm	NA	0.27 ± 0.89	NA
Dinoflagellate <20 μm	0.21 ± 0.30	-1.51 ± 0.54	-0.26 ± 0.15
Dinoflagellate 20-50 μm	0.26 ± 0.18	-1.20 ± 0.61	-0.22 ± 0.33
Dinoflagellate >50 μm	NA	0.10 ± 0.65	0.23 ± 0.51
Diatom <20 μm	0.42 ± 0.25	0.47 ± 0.18	-1.14 ± 0.71
Diatom 20-50 μm	0.76 ± 0.40	-1.11 ± 0.19	1.72 ± 1.03
Diatom >50 μm	0.14 ± 0.30	0.57 ± 0.31	0.23 ± 0.44
Chlorophyll *a*	0.11 ± 0.01	0.20 ± 0.73	0.41 ± 0.07

Regarding community grazing, measurements of chlorophyll *a* revealed occurrence at all stations and for all treatments (table 5). Grazing rates were generally higher in the samples were *C. glacialis* were added (0.015 ± 0.01 d^{-1}, $p < 0.001$, for DE110, 0.18 ± 0.68 d^{-1}, $p = 0.807$, for DE310 and 0.36 ± 0.08 d^{-1}, $p = 0.001$ for DE410) compared to those of solely protists (0.08 ± 0.01 d^{-1}, $p = 0.002$, for DE110, 0.09 ± 0.07 d^{-1}, $p = 0.900$, for DE310 and 0.27 ± 0.06 d^{-1}, $p = 0.013$, for DE410). For both treatments, the higher grazing rates were found at station DE410, followed by DE310, with the least grazing happening at station DE110.

Microscopy counts, revealed grazing on most of the groups at station DE110 (table 5). At this station, grazing on the alveolate groups were generally higher in samples exposed to *C. glacialis* (0.27 ± 0.28 and 0.14 ± 0.26 d^{-1} for ciliates of <20 μm and 20-50 μm, and 0.37 ± 0.31 and 0.44 ± 0.13 for dinoflagellates of <20 μm and 20-50 μm, respectively) compared to samples without copepods, where grazing only was observed on ciliates <20 μm (0.04 ± 0.29 d^{-1}) and dinoflagellates <20 μm and of 20-50 μm (0.29 ± 0.28 and 0.31 ± 0.17 d^{-1}, respectively). For diatoms on the other hand, higher grazing rates were seen in the samples without copepods (0.43 ± 0.24 d^{-1} for <20 μm, 0.66 ± 0.39 d^{-1} for 20-50 μm and 0.03 ± 0.25 d^{-1} for <50 μm, compared to 0.37 ± 0.20 d^{-1} for <20 μm and 0.41 ± 0.35 d^{-1} for 20-50 μm). No grazing was found on diatoms >50 μm.

At station DE310, there were no grazing on the alveolate groups <50 μm. However, some grazing occurred on ciliates >50 μm without copepods (0.10 ± 0.74 d^{-1}) and the dinoflagellates >50 μm of both treatments (0.61 ± 0.54 d^{-1} without copepods and 0.70 ± 0.11 d^{-1} with). At this station there were no grazing on diatoms between 20 and 50 μm. However, diatoms <20 μm were consumed in both the treatment without copepods and with (0.50 ± 0.18 and 1.09 ± 0.17 d^{-1}, respectively). So were the diatoms >50 μm (0.07 ± 0.30 without and 0.17 ± 0.33 d^{-1} with copepods). For both these diatom groups, higher grazing rates were seen where copepods were added.

Furthermore, there was no observed grazing on alveolates at station DE410 with the exception being the ciliates <20 μm (0.17 ± 0.19 d^{-1} without copepods and 0.31 ± 0.23 d^{-1} with) and the dinoflagellates >50 μm (0.50 ± 0.59 d^{-1} without copepods). Regarding diatoms, no grazing was documented on the individuals <20 μm for either treatment. For the other two diatom size groups, there were more grazing on individuals between 20 and 50 μm (0.73 ± 0.43 d^{-1} with copepods and 1.34 ± 0.86 d^{-1} without) and some grazing on individuals above 50 μm (0.03 ± 0.32 d^{-1} with copepods and 0.63 ± 0.42 d^{-1} without). For both these diatom groups, higher grazing rates were observed for the treatments without copepods.

Table 5: Grazing rates of the experimental groups. Here measured per day over the course of 48-65 h for samples with and without copepods. Green indicates that grazing occurred, and darker shades reflect higher grazing rates. Where estimates were not available (NA), cells are marked in grey. Grazing occurred on most diatom groups and fewer of the dinoflagellate and ciliate ones. Station DE110, however, had grazing on most groups.

Grazing rates (d^{-1})						
	DE110		**DE310**		**DE410**	
Group	**100%**	**Cop**	**100%**	**Cop**	**100%**	**Cop**
Ciliate <20 μm	0.04 ± 0.29	0.27 ± 0.28	0.00	0.00	0.17 ± 0.19	0.31 ± 0.23
Ciliate 20-50 μm	0.00	0.14 ± 0.26	0.00	0.00	0.00	0.00
Ciliate >50 μm	NA	NA	0.10 ± 0.74	NA	NA	NA
Dinoflagellate <20 μm	0.29 ± 0.28	0.37 ± 0.31	0.00	0.00	0.00	0.00
Dinoflagellate 20-50 μm	0.31 ± 0.17	0.44 ± 0.13	0.00	0.00	0.00	0.00
Dinoflagellate >50 μm	NA	NA	0.61 ± 0.54	0.70 ± 0.11	0.50 ± 0.59	NA
Diatom <20 μm	0.43 ± 0.24	0.37 ± 0.20	0.50 ± 0.18	1.09 ± 0.17	0.00	0.00
Diatom 20-50 μm	0.66 ± 0.39	0.41 ± 0.35	0.00	0.00	1.34 ± 0.86	0.73 ± 0.43
Diatom >50 μm	0.03 ± 0.25	0.00	0.07 ± 0.30	0.17 ± 0.33	0.63 ± 0.42	0.03 ± 0.32
Chlorophyll *a*	0.08 ± 0.01	0.15 ± 0.01	0.09 ± 0.07	0.18 ± 0.68	0.27 ± 0.06	0.36 ± 0.08

3.5 Planktoscope

Analyses by the Planktoscope did not give abundance estimates in any of the samples. No individuals were detected by the camera system when segmenting the sample footage. However, a few individuals could be seen when running the whole sample through at the low flow through rate of 0.005 mL/pump. Screenshots taken of these individuals represent the resolution and focus of the system (figure 15).

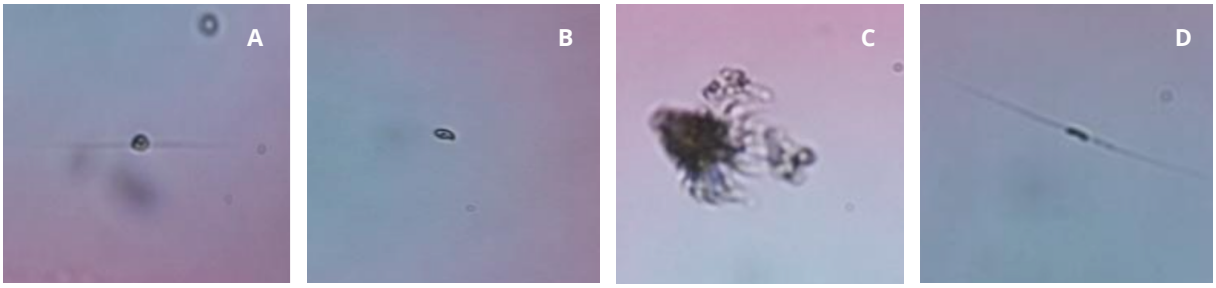

Figure 15: Phytoplankton images from the Planktoscope. Plankton were not detected by the device itself, and therefore documented as screenshots of the Planktoscope display window – hence scale is not defined. The individuals displayed were from a sample incubated with *C. glacialis* at station DE110. A) Diatom. B) Dinoflagellate. C) Ciliate. D) Diatom.

4 Discussion

4.1 Environmental conditions

Samples for this project were collected during the fall of 2021 between the 13th and 20th of October (table 1). At the time of sampling, no sea-ice had formed in Baffin Bay. A "typical ice year" for this area, is characterized by sea-ice formation from September in the north, which spreads south, with a sea-ice maximum reached in March. Interannual differences in sea-ice extent have further been found to be tightly coupled to atmospheric temperatures (Tang *et al.*, 2004 & references therein). Metrological data from 2021 establishes a temperature anomaly for October in northern Canada with some areas of Nunavut, where Baffin Bay is located, experiencing temperatures of 7 °C above average (1991-2020) (figure 1) (The Copernicus Programme, 2021). It is therefore likely that the observed aberration in ice conditions were caused by abnormally warm atmospheric temperatures for this particular fall.

Regarding thermohaline conditions, the water masses identified by CTD-data were mostly within the temperature and salinity ranges of what has previously been described for the area (see section 3.1) (Addison & Bourke, 1987; Coachman & Aagaard, 1974; Fissel *et al.*, 1982; Aagaard & Coachman, 1968). The only exceptions were the sub-zero temperatures observed in the mixed layer (figure 7-9). Due to its direct contact with air, this layer is highly affected by atmospheric temperatures, and therefore sub-zero cooling is expected during fall. The observed mixed layer was also quite fresh – in agreement with a potential surface freshening as described by Yamamoto-Kawai *et al.*(2009) for other parts of the Canadian Arctic.

It should further be noted that a study by Zweng & Münchow (2006), conducted between 1916 and 2003, found that the parts of Baffin Bay influenced by the West Greenland Current have been subject to a significant warming. Such warming was however not seen for this project where temperatures generally stayed around 0 °C below 300 m – lower than what was reported by the study (>1 °C at the temperature maximum of 500 m) (Zweng & Münchow, 2006). A potential cause of divergence may however be that samples for this project were taken further north in areas with a higher influence of colder Arctic water (Tang *et al.*, 2004).

The nutrient conditions in northern Baffin Bay are dependent on both physical and biological processes. The highest nutrient concentrations occur during winter due to mixing breaking stratification – followed by utilization during phytoplankton blooms from May to September (Booth *et al.*, 2002; Tremblay *et al.*, 2002). Nitrate has been documented as the yield-limiting nutrient in northern Baffin Bay during conditions similar to those of this project. Yet, silica can be limiting with lower inflow of Arctic water with origin from the Bering Sea (Tremblay *et al.*, 2002). The nitrate (0.49 to 2.13 μM) and silicate (0.96 to 4.25 μM) concentrations observed in this project were depleted in comparison to pre-bloom conditions (10-11 μM for nitrate and 11.6-24 μM for silicate), indicating that the productive period of phytoplankton was coming to an end (table 3). Nitrate was however not fully exhausted (<0.05 μM) and may therefore have still support some production (Tremblay *et al.*, 2002).

4.2 Protist community composition

The samples for this project revealed a high relative abundance of dinoflagellates (63-71%) in northern Baffin Bay during the fall of 2021 (figure 13). These were mostly seen in athecate forms. Diatoms showed relative abundances of 22-30% with a dominance of *Chaetoceros* spp. at station DE110 and DE410, and *Leptocylindrus* spp. at station DE310. Ciliates were least abundant, making up 7-11% of mainly oligotrich forms.

These results were somewhat contrasting to earlier descriptions of northern Baffin Bay as a system dominated by diatoms. A study by Lovejoy *et al.* (2002), conducted in 1998, for instance found diatoms to account for 70% of the total biomass of the community, with dinoflagellates and ciliates comprising 24%, in the period of April to July. In this study *Thalassiosira* spp., *Porosira* spp. and *Chaetoceros* spp. were the dominant genera – responsible for the spring and summer blooms of the area. However, a seasonal succession was observed where the relative biomass of dinoflagellates and ciliates increased when the phytoplankton blooms passed (Lovejoy *et al.*, 2002). An extension of this succession could therefore explain the dominance of dinoflagellates in October. This is however contradicted by observations of the plankton community in northern Baffin Bay during the fall of 2006, where diatoms were found to account for >50% of total protist abundance (Blais *et al.*, 2017).

Furthermore, the samples for this project also revealed a larger contribution from smaller individuals <20 μm in the total abundance of the community. They made up 82-87% of all dinoflagellates and 63-68% of all ciliates. Regarding diatoms they made up 85% and 96% for station DE410 and DE110 respectively, with station DE310 being the only station with a dominance of diatoms between 20-50 μm (83%). Contradictory, the planktonic community in northern Baffin Bay has been observed to consist of mainly larger protist cells in the size range of 20-200 μm (Lovejoy *et al.*, 2002). Thus, there was a gap between both the taxonomic and dimensional community composition found in this project, compared to the observed composition in studies conducted around the turn of the century.

Distribution of phytoplankton biomass is mainly defined by the availability of light and nutrients, again determined by physical parameters such as mixed layer-dynamics, ocean circulation, atmospheric conditions and the solar cycle (Ardyna *et al.*, 2011; Sakshaug & Slagstad, 1991). Freshwater input is tightly linked to stratification of surface waters in the Arctic ocean due to its low density (Aagaard & Coachman, 1968). Over the past decades the combined effects of increased precipitation and melt-water input has therefore led to an increase in stratification of surface waters in the Canada Basin (Serreze *et al.*, 2009; Yamamoto-Kawai *et al.*, 2009).

Diatom-based systems are found to be associated with well-mixed, saline waters, repleted with inorganic nitrogen, as previously found in northern Baffin Bay. Thus, the stratification observed over the last decades may lead to governed supply of nutrients to surface waters and alternate community composition (Ardyna *et al.*, 2011). This was seen in a multi-year study conducted during the fall of 1999-2011 where centric diatom abundance was seen to decrease from >50% to 10% (Blais *et al.*, 2017). At the end of the study period the phytoplankton community was numerically dominated by flagellated cells (including dinoflagellates). Furthermore, stratification and lower nutrient availability

has been found to give smaller cells a competitive advantage due to their more efficient nutrient uptake and lower susceptibility to gravitational settling (Li *et al.*, 2009). This is further supported by a major shift in community size structure, towards smaller individuals, observed from 1999-2011 in northern Baffin Bay during fall (Blais *et al.*, 2017). Both these observations are in agreement with what was seen in this project.

Additionally, larger cells have been found to perform better than smaller ones at higher light intensities (Pesant *et al.*, 1996). Hence, the community observed in this project is typical for a light-limited system during late fall, as supported by other studies in the Canadian Arctic (Simo-Matchim *et al.*, 2016). However, considering the ice-free conditions and low nutrient concentrations for this project, it is more likely that the observed community composition was a result of low nutrient availability caused by a stratified surface.

4.3 Growth and grazing rates

Phytoplankton was generally found to have positive growth rates in northern Baffin Bay during the fall of 2021. Growth rates based on chlorophyll *a* concentrations here ranged between 0.11 ± 0.01 and 0.41 ± 0.07 cell div. d^{-1} (table 4). A study by Paranjape, (1987) conducted in northern Baffin Bay, during post-bloom conditions in 1983, shows similar values. For 12th and 13th of September, rates of 0.19 ± 0.03 and 0.29 ± 0.03 d^{-1} were seen in the area – corresponding to 0.28 and 0.41 cell div. d^{-1} . In this previous study, nutrient limitation was however accounted for by adding nitrate to the incubation bottles. It is thus not fully representative of *in situ* rates if a limitation was present (Paranjape, 1987).

The picture painted by chlorophyll *a* was further nuanced by growth rates estimated for different size classes of diatoms – the dominating taxa in primary production of the western Arctic Ocean (table 4)(Gosselin *et al.*, 1997; Tremblay *et al.*, 2002). Among diatoms, growth was seen for all size classes except 20-50 μm at station DE310 and <20 μm at station DE410, which were the most numerous size classes at these stations (figure 13). The negative growth rates and high abundances observed suggest that a period of growth had ended for *Chaetoceros* spp. at station DE410 and *Leptocylindrus* spp. at station DE310, with mortality rates exceeding growth rates. A persistence of both these genera has previously been seen to last until fall in the area (Blais *et al.*, 2017), and such results may thus be expected. Yet, nutrient and light conditions seemed to support growth for the rest of the diatom groups. At station DE110, for instance, positive growth rates accompanied by low nitrate (0.49 ± 0.02 μM) and silicate (0.96 ± 0.00μM) concentrations indicate that a period of growth might be coming to an end. Furthermore, the high concentrations of nitrate (2.13 ± 0.02 μM) and silicate (4.25 ± 0.01) at station DE410 may have given larger cells a competitive advantage (Ardyna *et al.*, 2011), potentially explaining the positive growth of diatoms >20 μm.

Quite low to negative growth rates were generally seen for ciliates and dinoflagellates <50 μm (table 4) – which were the numerically dominating size classes of these taxa (figure 13). This is in agreement with previous findings that low temperatures, as generally seen during the Arctic fall, constrain growth of heterotrophic protists (Rose & Caron, 2007). Protist growth rates may here be constrained to an extent where their maximum growth rates are half of what is seen for phototrophic protists, due to the effect of temperature on metabolism (Brown *et al.*, 2004; López-Urrutia, 2008). Low and

negative growth rates may also be explained by seasonal progression where the decrease in the numerically dominant diatom groups at station DE310 and DE410 lower food availability. This is supported by findings of a strong correlation between biomass of phytoplankton and microzooplankton (Sherr *et al.*, 2009). An exception, however, occurred at station DE110 where dinoflagellates <50 μm and all diatom groups had positive growth rates, suggesting that production by *Chaetoceros* spp. in this area, still supported dinoflagellate growth.

Grazing on phytoplankton was also found during the sample period (table 5). Grazing rates, based on chlorophyll *a* measurements, here ranged between 0.08 ± 0.01 and 0.27 ± 0.06. These values also correspond to the values observed by Paranjape (1987) in September, 1983, where grazing rates were found to be 0.12 ± 0.02 and 0.17 ± 0.04 d^{-1} in the Jones Sound and northern Baffin Bay, respectively. Grazing pressure was further found to be higher at each station in 2021 with addition of *C. glacialis* – giving rates of 0.15 ± 0.01 to 0.36 ± 0.08 d^{-1}. This result is expected as phytoplankton has been documented as the main prey item of this copepod species (Campbell *et al.*, 2009).

When looking at grazing on different size classes of diatoms, no clear trends were observed. Grazing rates both varied within stations for different size classes and between stations for the same size class – with and without the addition of *C. glacialis*. This may suggest a general absence of size selection by the grazers. Random feeding, in regard to size, is supported by descriptions of heterotrophic dinoflagellates as non-selective feeders able to engulf prey items larger than themselves (Sherr & Sherr, 2007). Calanoid copepods are further found to feed non-selectively when food is scarce (Cleary *et al.*, 2017; Cowles, 1979). Ciliates, on the other hand, are known to be more selective with a typical predator-prey size ratio of 10:1. However, due to their relatively low abundances compared to dinoflagellates, this effect does not seem to be major.

It also varied whether addition of *C. glacialis* increased or reduced the grazing pressure of diatoms. At station DE110 tendencies of top-down control were seen, with higher consumption of alveolates and lower of diatoms in the treatment with copepods. This is in agreement with previous experiments on mesozooplankton grazing, in the western Arctic Ocean, revealing heterotrophic protists to be preferred over phytoplankton as prey, when available (Li *et al.*, 2009). By reducing alveolate grazer abundances they may therefore reduce grazing pressure of phytoplankton (Hirche *et al.*, 1991). Contradictory, station DE310 and DE410 had no observed consumption of most heterotrophic groups. At the prior station, the addition of *C. glacialis* added to the grazing pressure of diatoms but not at the latter. Thus, there were no clear trends in how these copepods affected the protist community dynamics in samples for this project. This suggests that feeding by *C. glacialis* was quite random at the time of sampling, as previously observed during low food availability in other studies (Cleary *et al.*, 2017; Cowles, 1979).

4.4 Methodological considerations

The dilution method is a simple way of attaining growth and grazing rates as it avoids excessive manipulation of the protist community (Paranjape, 1987). The method has been proven accurate and is widely used in assessing plankton community dynamics (Landry *et al.*, 1995; M. R. Landry & Hassett, 1982; Sherr *et al.*, 2009). There are, however, some implications of this method such as the potential for loss of material during collection and handling. Exposure to high light intensities has for instance been

found to cause phytoplankton bleaching in another study at high latitudes (Caron *et al.*, 2000) and exposure to air bubbles may lyse particular protists (Gifford, 1988). Another factor that may introduce a bias with this method is the potential for nutrient limitation of phytoplankton growth during incubation in a closed environment (M. R. Landry, 1993). Furthermore initially screening samples over 180 μm mesh is likely to have excluded particularly large protists such as *Tripos* spp. – underestimating their relative contribution. These factors may therefore have introduced some bias to this project.

It should further be addressed that due to capacity constraints, only two replicates for each treatment were counted in the microscope. This may amplify the effect of random errors and make estimates of growth and grazing less accurate. Sample size also varied greatly between size classes making estimates of numerically dominant groups (typically <20 μm) more accurate than those of fewer individuals (typically >50 μm). Estimates based on chlorophyll *a* concentrations were however based on a larger sample size and thus more significant.

Furthermore, Utermöhl sedimentation was used for the microscopic analyses in this project (figure 4). This method gives the advantage of allowing visualization of the whole protist community – using one technique. While morphological differences may be too vague to distinguish protists down to a species level, most of them can be found to belong to a particular taxon (Lovejoy *et al.*, 2002). Some bias may, however, be introduced by clumping and potential loss over time due to degradation (Anderson & Karlson, 2017). Additionally, functional traits such as if species were autotroph or heterotroph were not accounted for (Sherr & Sherr, 1993).

4.5 Planktoscope

To obtain optimal results from the Planktoscope, multiple adjustments and setting were tested (detailed in section 2.4). Nevertheless, analyses by the Planktoscope did not give estimates of plankton abundances as individuals were not detected by the system. The lack of detection is likely due to a combination of factors including plankton settling, low protist concentration in samples, poor camera resolution and a fixed focus.

Micro- and nanoplankton cells, including protists, are subject to larger gravitational forces than smaller cells and therefore prone to settlement (Li *et al.*, 2009). Settlement in the system is thus likely to occur if pumping velocity, and thereby suspension, is low. When attaining higher pumping velocities, the system only captures a portion of the sample. This trade-off between suspension and sample coverage, was in this project taken into account by running samples at multiple pumping velocities – yet with no detection of plankton.

Introducing a camera to microscopy also compromises resolution, which makes it harder to spot vague, morphological distinctions. This may be the case for both the human eye and artificial intelligence (Benfield *et al.*, 2007). When samples were run through the Planktoscope, no segmented images were recognized by EcoTaxa algorithms, potentially for this reason. Additionally, plankton comprise a significantly heterogenic group, particularly in terms of size (Schmidt *et al.*, 2006). Therefore, the fixed focus of the Planktoscope was not optimal in capturing plankton that for this project ranged between 10-500 μm. Hence, some material may have been out of focus and therefore not detected.

Nevertheless, the novel Planktoscope has successfully portrayed qualitative plankton composition in a previous study (Mériguet *et al.*, 2022). In this study, sampling was performed with a plankton net instead of a Niskin bottle. With the potential for collecting specimens of large water column transects, plankton nets often provide dense samples. This method may, however, compromise accuracy of plankton quantities and relative contribution (Jiang *et al.*, 2020). Contrasting, samples obtained by Niskin bottles represent composition of the *in situ* community. Despite concentration through Utermöhl sedimentation and filtering, the samples for this project seemed to contain insufficient amounts of cells for the Planktoscope to be efficient. Measures for increasing plankton densities while also ensuring accuracy of relative abundance could therefore improve the experimental approach of this project further.

It should also be noted that some refinements could be added to improve the overall functioning of the Planktoscope. To counteract settlement, other video microscopes have successfully implemented acoustic waves that center particles in samples, such as the FlowCytobot (Olson *et al.*, 2017). Additionally, an automated focus and higher resolution camera could improve detection (Yang & Luo, 2008). Such additions would however drastically increase the cost and complexity of this device – compromising two of its biggest strengths.

4.6 Future perspectives

As subject to arctic amplification, northern Baffin Bay is going through rapid environmental changes. Ice-melt and runoff are freshening and stratifying surface waters while deeper Atlantic water of the West Greenland Current is getting warmer (Zweng & Münchow, 2006). Environmental forces may further shape the base of the food web through altering plankton community composition and trophic dynamics (Blais *et al.*, 2017).

Tendencies of an alternated plankton community are already seen in the area. The relative contribution of large diatoms have for instance been drastically reduced over the latest century accompanied by an increase in smaller flagellated cells (Blais *et al.*, 2017). These observations are further supported by this project. The observations may imply that northern Baffin Bay is undergoing a shift towards a more oligotrophic, flagellate-based system as seen in the Beaufort Sea – due to increased stratification (Ardyna *et al.*, 2011). Such a shift could greatly limit the food export to higher trophic levels during fall due to the small size of phytoplankton (Pesant *et al.*, 1996) and thus impair the local ecosystem.

A shift towards a more oligotrophic system is further supported by a drastic decrease in primary production observed during the fall of 1999 to 2011 (Blais *et al.*, 2017). This suggests a decrease in overall phytoplankton growth in northern Baffin Bay over the years. Such a decrease was not supported by comparison of phytoplankton growth rates during the fall of 1983 and 2021 (Paranjape, 1987). Growth is, however, a highly fluctuating measure strongly dependent on momentary conditions. This was also seen by Paranjape (1987), where growth rates of phytoplankton increased significantly over the course of two weeks due to a mixing event in the Jones Sound. Hence, this parameter gives poor indications of overall trends in a changing environment when not measured

over extensive periods. There is also generally a lack of baseline studies in northern Baffin Bay, to compare with.

Grazing rates are tightly connected to growth and thus also quite fluctuating (Schmoker *et al.*, 2013). It is likely that a warming ocean could alter this intricate balance (Chen *et al.*, 2012). An expected direct effect of a warmer environment is an increase in growth rates of microzooplankton due to enhanced metabolism. This may further strengthen the top-down control of phytoplankton through grazing (Rose & Caron, 2007). However, more research is needed on the role of microzooplankton in high-latitude Arctic food-webs (Yang *et al.*, 2015), especially in regard to climate change (Caron & Hutchins, 2013).

The Planktoscope is a device that could enable such extensive monitoring of plankton ecosystems and thus contribute in assessing effects of climate change on protist community dynamics (Pollina *et al.*, 2022). However, it requires some upgrades to determine quantities of plankton in water samples more accurately. Suggestions for future improvements are therefore to implement an automated focus, a higher resolution camera and methods to avoid plankton settlement such as acoustic waves (Olson *et al.*, 2017; Yang & Luo, 2008). As of now, the device is found to perform better in qualitative analyses (Mériguet *et al.*, 2022), than quantitative ones – as for this project. Yet, it has potential in extension of quantitative analyses. By revealing plankton community composition it could for instance improve understanding of *in situ* conditions when estimating growth and grazing rates based on chlorophyll *a* concentrations.

5 Concluding remarks

The protist community composition of northern Baffin Bay was found to differ from earlier descriptions. The most striking differences were the decrease in relative abundance of diatoms as well as a shift towards smaller cells, as also found in other studies. These findings might be explained by seasonal succession and fall conditions. However, an observed stratified mixed layer and low nutrient concentrations, in agreement with recent trends seen for the area, suggest that climate change could be a factor.

In regard to growth and grazing dynamics, less distinct differences were seen in comparison to the fall of 1983. The area was characterized by some phytoplankton growth while microzooplankton showed low to negative growth rates. The findings witnessed a transition to post-bloom conditions. Grazing both by microzooplankton and copepods occurred in the area, mostly on diatoms, and with little selectivity. Low feeding selectivity is a trait further associated with low food availability for copepods, in agreement with studies showing a drastic decrease in primary production of the area over the years. This also suggests that phytoplankton growth is generally decreasing. To be able to draw conclusions on how grazing dynamics could respond to these changes, more comprehensive studies are needed. It is however hypothesized that increasing temperature and thus metabolic activity could increase top-down control by heterotrophic protists.

The Planktoscope was not proven accurate in assessment of the plankton community dynamics of northern Baffin Bay with this experimental set-up. It might, however, have potential for denser samples and do better in qualitative analyses. Yet, improvements of focus, resolution and suspension of samples could be necessary for this device to reach its full potential.

References

Addison, V. G., & Bourke, R. H. (1987). The physical oceanography of the northern Baffin Bay-Nares Strait region. Naval Postgraduate School. https://doi.org/10.5962/bhl.title.62158

Aksu, A. E., & Piper, D. J. W. (1979). Baffin Bay in the past 100,000 yr. *Geology*, *7*(5), 245–248. https://doi.org/10.1130/0091-7613(1979)7<245:BBITPY>2.0.CO;2

Amundsen Science Data Collection. 2021. CTD-Rosette data collected by the CCGS Amundsen in the Canadian Arctic. Arcticnet Inc., Québec, Canada. Processed data. Version 1. Archived at www.polardata.ca, Canadian Cryospheric Information Network (CCIN), Waterloo, Canada. https://doi: 10.5884/12713. Accessed on 01.11.2021.

Anderson, D. M., & Karlson, B. (2017). Preservatives and methods for algal cell enumeration. I *Harmful Algal Blooms (HABs) and Desalination: A Guide to Impacts, Monitoring, and Management*, 509-519. Intergovernmental Oceanographic Commission.

Ardyna, M., & Arrigo, K. R. (2020). Phytoplankton dynamics in a changing Arctic Ocean. *Nature Climate Change*, *10*(10), 892–903. https://doi.org/10.1038/s41558-020-0905-y

Ardyna, M., Gosselin, M., Michel, C., Poulin, M., & Tremblay, J. É. (2011). Environmental forcing of phytoplankton community structure and function in the Canadian High Arctic: Contrasting oligotrophic and eutrophic regions. *Marine Ecology Progress Series*, *442*, 37–57. https://doi.org/10.3354/meps09378

Arrigo, K. R., van Dijken, G., & Pabi, S. (2008). Impact of a shrinking Arctic ice cover on marine primary production. *Geophysical Research Letters*, *35*(19). https://doi.org/10.1029/2008GL035028

Ballinger, T. J., Moore, G. W. K., Garcia-Quintana, Y., Myers, P. G., Imrit, A. A., Topál, D., & Meier, W. N. (2022). Abrupt Northern Baffin Bay Autumn Warming and Sea-Ice Loss Since the Turn of the Twenty-First Century. *Geophysical Research Letters*, *49*(21). https://doi.org/10.1029/2022GL101472

Benfield, M. C., Grosjean, P., Culverhouse, P. F., Irigoien, X., Sieracki, M. E., Lopez-Urrutia, A., Dam, H. G., Hu, Q., Davis, C. S., Hansen, A., Pilskaln, C. H., Riseman, E. M., Schultz, H., Utgoff, P. E., & Gorsky, G. (2007). RAPID: Research on Automated Plankton Identification. *Oceanography (Washington, D.C.)*, *20*(2), 172–187. https://doi.org/10.5670/oceanog.2007.63

Blais, M., Ardyna, M., Gosselin, M., Dumont, D., Bélanger, S., Tremblay, J. É., Gratton, Y., Marchese, C., & Poulin, M. (2017). Contrasting interannual changes in phytoplankton productivity and community structure in the coastal Canadian Arctic Ocean. *Limnology and Oceanography*, *62*(6), 2480–2497. https://doi.org/10.1002/lno.10581

Booth, B. C., Larouche, P., Bélanger, S., Klein, B., Amiel, D., & Mei, Z.-P. (2002). Dynamics of *Chaetoceros socialis* blooms in the North Water. *Deep Sea Research Part II: Topical Studies in Oceanography*, *49*(22), 5003–5025. https://doi.org/10.1016/S0967-0645(02)00175-3

Brown, J. H., Gillooly, J. F., Allen, A. P., Savage, V. M., & West, G. B. (2004). Toward a Metabolic Theory of Ecology. *Ecology*, *85*(7), 1771–1789. https://doi.org/10.1890/03-9000

Campbell, R. G., Sherr, E. B., Ashjian, C. J., Plourde, S., Sherr, B. F., Hill, V., & Stockwell, D. A. (2009). Mesozooplankton prey preference and grazing impact in the western Arctic Ocean. *Deep Sea Research Part II: Topical Studies in Oceanography*, *56*(17), 1274–1289. https://doi.org/10.1016/j.dsr2.2008.10.027

Caron, D. A., Dennett, M. R., Lonsdale, D. J., Moran, D. M., & Shalapyonok, L. (2000). Microzooplankton herbivory in the Ross Sea, Antarctica. *Deep Sea Research Part II: Topical Studies in Oceanography*, *47*(15), 3249–3272. https://doi.org/10.1016/S0967-0645(00)00067-9

Caron, D. A., & Hutchins, D. A. (2013). The effects of changing climate on microzooplankton grazing and community structure: Drivers, predictions and knowledge gaps. *Journal of Plankton Research*, *35*(2), 235–252. https://doi.org/10.1093/plankt/fbs091

Chen, B. (2015). Assessing the accuracy of the "two-point" dilution technique. *Limnology and Oceanography: Methods*, *13*(10), 521–526. https://doi.org/10.1002/lom3.10044

Chen, B., Landry, M. R., Huang, B., & Liu, H. (2012). Does warming enhance the effect of microzooplankton grazing on marine phytoplankton in the ocean? *Limnology and Oceanography*, *57*(2), 519–526. https://doi.org/10.4319/lo.2012.57.2.0519

Cleary, A. C., Søreide, J. E., Freese, D., Niehoff, B., & Gabrielsen, T. M. (2017). Feeding by Calanus glacialis in a high arctic fjord: Potential seasonal importance of alternative prey. *ICES Journal of Marine Science*, *74*(7), 1937–1946. https://doi.org/10.1093/icesjms/fsx106

Coachman, L. K., & Aagaard, K. (1974). Physical Oceanography of Arctic and Subarctic Seas, *Marine Geology and Oceanography of the Arctic Seas*, *13*(3), 1–72. https://doi.org/10.1007/978-3-642-87411-6_1

Cooley, S. W., Ryan, J. C., Smith, L. C., Horvat, C., Pearson, B., Dale, B., & Lynch, A. H. (2020). Coldest Canadian Arctic communities face greatest reductions in shorefast sea ice. *Nature Climate Change*, *10*(6), 533–538. https://doi.org/10.1038/s41558-020-0757-5

Copernicus Climate Change Service. (2021). *Surface air temperature for October 2021.* Retrieved May 2, 2024, from https://climate.copernicus.eu/surface-air-temperature-october-2021

Cowles, T. (1979). The feeding response of copepods from the Peru upwelling system: Food size selection. *Journal of Marine Research*, *37*(3). https://elischolar.library.yale.edu/journal_of_marine_research/1486

Culverhouse, P. F., Williams, R., Reguera, B., Herry, V., & González-Gil, S. (2003). Do experts make mistakes? A comparison of human and machine indentification of dinoflagellates. *Marine Ecology Progress Series*, *247*, 17–25. https://doi.org/10.3354/meps247017

Davis, C. S., Gallager, S. M., Marra, M., & Kenneth Stewart, W. (1996). Rapid visualization of plankton abundance and taxonomic composition using the Video Plankton Recorder. *Deep Sea Research Part II: Topical Studies in Oceanography*, *43*(7), 1947–1970. https://doi.org/10.1016/S0967-0645(96)00051-3

Falk-Petersen, S., Pavlov, V., Timofeev, S., & Sargent, J. R. (2007). Climate variability and possible effects on arctic food chains: The role of Calanus. I J. B. Ørbæk, R. Kallenborn, I. Tombre, E. N. Hegseth, S. Falk-Petersen, & A. H. Hoel (Eds.), *Arctic Alpine Ecosystems and People in a Changing Environment*, 147–166, https://doi.org/10.1007/978-3-540-48514-8_9

Fissel, D. B., Lemon, D. D., & Birch, J. R. (1982). Major Features of the Summer Near-Surface Circulation of Western Baffin Bay, 1978 and 1979. *Arctic*, *35*(1), 180–200. https://doi.org/10.14430/arctic2318

Franzé, G., & Modigh, M. (2013). Experimental evidence for internal predation in microzooplankton communities. *Marine Biology*, *160*(12), 3103–3112. https://doi.org/10.1007/s00227-013-2298-1

Garcia, T. M., Costa, A. C. P., Campos, C. C., Júnior, J., Barroso, H. S., & Soares, M. de O. (2022). The Decade of Ocean Science: The Importance of «Rediscovering» the Tiny and Invisible World of Plankton. *Arquivos de Ciências Do Mar*, *55*(Special), Artikkel Special. https://doi.org/10.32360/acmar.v55iEspecial.78407

Gifford, D. J. (1988). Impact of grazing by microzooplankton in the Northwest Arm of Halifax Harbour, Nova Scotia. *Marine Ecology Progress Series*, *47*(3), 249–258.

Gosselin, M., Levasseur, M., Wheeler, P. A., Horner, R. A., & Booth, B. C. (1997). New measurements of phytoplankton and ice algal production in the Arctic Ocean. *Deep Sea Research Part II: Topical Studies in Oceanography*, *44*(8), 1623–1644. https://doi.org/10.1016/S0967-0645(97)00054-4

Harrison, W. G. (1980). Nutrient Regeneration and Primary Production in the Sea. I P. G. Falkowski (Eds.), *Primary Productivity in the Sea*, 433–460. Springer US. https://doi.org/10.1007/978-1-

4684-3890-1_24

Hays, G. C., Richardson, A. J., & Robinson, C. (2005). Climate change and marine plankton. *Trends in Ecology & Evolution*, *20*(6), 337–344. https://doi.org/10.1016/j.tree.2005.03.004

Hirche, H.-J., Baumann, M. E. M., Kattner, G., & Gradinger, R. (1991). Plankton distribution and the impact of copepod grazing on primary production in Fram Strait, Greenland Sea. *Journal of Marine Systems*, *2*(3), 477–494. https://doi.org/10.1016/0924-7963(91)90048-Y

Hobson, K. A., Fisk, A., Karnovsky, N., Holst, M., Gagnon, J.-M., & Fortier, M. (2002). A stable isotope (δ13C, δ15N) model for the North Water food web: Implications for evaluating trophodynamics and the flow of energy and contaminants. *Deep Sea Research Part II: Topical Studies in Oceanography*, *49*(22), 5131–5150. https://doi.org/10.1016/S0967-0645(02)00182-0

Holst, M., Stirling, I., & Hobson, K. A. (2001). Diet of Ringed Seals (phoca Hispida) on the East and West Sides of the North Water Polynya, Northern Baffin Bay. *Marine Mammal Science*, *17*(4), 888–908. https://doi.org/10.1111/j.1748-7692.2001.tb01304.x

Jiang, Z., Liu, J., Zhu, X., Chen, Y., Chen, Q., & Chen, J. (2020). Quantitative comparison of phytoplankton community sampled using net and water collection methods in the southern Yellow Sea. *Regional Studies in Marine Science*, *35*, 10125. https://doi.org/10.1016/j.rsma.2020.101250

Karnovsky, N. J., & Hunt, G. L. (2002). Estimation of carbon flux to dovekies (*Alle alle*) in the North Water. *Deep Sea Research Part II: Topical Studies in Oceanography*, *49*(22), 5117–5130. https://doi.org/10.1016/S0967-0645(02)00181-9

Kirchman, D. L., Morán, X. A. G., & Ducklow, H. (2009). Microbial growth in the polar oceans—Role of temperature and potential impact of climate change. *Nature Reviews Microbiology*, *7*(6), 451–459. https://doi.org/10.1038/nrmicro2115

Landry, M., Haas, L., & Fagerness, V. (1984). Dynamics of microbial plankton communities: Experiments in Kaneohe Bay, Hawaii. *Marine Ecology*, *16*, 127–133. https://doi.org/10.3354/meps016127

Landry, M. R. (1993). Estimating Rates of Growth and Grazing Mortality of Phytoplanlcton by the Dilution Method. I *Handbook of Methods in Aquatic Microbial Ecology*. CRC Press.

Landry, M. R., & Hassett, R. P. (1982). Estimating the grazing impact of marine micro-zooplankton. *Marine Biology*, *67*(3), 283–288. https://doi.org/10.1007/BF00397668

Landry, R, M., Kirshtein, & Constantinou. (1995). A refined dilution technique for measuring the community grazing impact of microzooplankton, with experimental tests in the central equatorial Pacific. *Marine Ecology Progress Series*, *120*, 53–63. https://doi.org/10.3354/meps120053

Lawrence, C., & Menden-Deuer, S. (2012). Drivers of protistan grazing pressure: Seasonal signals of plankton community composition and environmental conditions. *Marine Ecology Progress Series*, *459*, 39–52. https://doi.org/10.3354/meps09771

Levinsen, H., & Nielsen, T. G. (2002). The trophic role of marine pelagic ciliates and heterotrophic dinoflagellates in arctic and temperate coastal ecosystems: A cross-latitude comparison. *Limnology and Oceanography*, *47*(2), 427–439. https://doi.org/10.4319/lo.2002.47.2.0427

Levitus, S., Antonov, J. I., Boyer, T. P., & Stephens, C. (2000). Warming of the World Ocean. *Science*, *287*(5461), 2225–2229. https://doi.org/10.1126/science.287.5461.2225

Li, W. K. W., McLaughlin, F. A., Lovejoy, C., & Carmack, E. C. (2009). Smallest Algae Thrive As the Arctic Ocean Freshens. *Science*, *326*(5952), 539–539. https://doi.org/10.1126/science.1179798

López-Urrutia, Á. (2008). The metabolic theory of ecology and algal bloom formation. *Limnology and Oceanography*, *53*(5), 2046–2047. https://doi.org/10.4319/lo.2008.53.5.2046

Lovejoy, C., Legendre, L., Martineau, M.-J., Bâcle, J., & von Quillfeldt, C. H. (2002). Distribution of phytoplankton and other protists in the North Water. *Deep Sea Research Part II: Topical Studies in*

Oceanography, *49*(22), 5027–5047. https://doi.org/10.1016/S0967-0645(02)00176-5

Luo, J. Y., Irisson, J.-O., Graham, B., Guigand, C., Sarafraz, A., Mader, C., & Cowen, R. K. (2018). Automated plankton image analysis using convolutional neural networks. *Limnology and Oceanography: Methods*, *16*(12), 814–827. https://doi.org/10.1002/lom3.10285

Manabe, S., & Wetherald, R. T. (1975). The Effects of Doubling the CO2 Concentration on the climate of a General Circulation Model. *Journal of the Atmospheric Sciences*, *32*(1), 3–15. https://doi.org/10.1175/1520-0469(1975)032<0003:TEODTC>2.0.CO;2

Meier, W. N., Stroeve, J., & Gearheard, S. (2006). Bridging perspectives from remote Sensing and Inuit communities on changing Sea-ice cover in the Baffin Bay region. *Annals of Glaciology*, *44*, 433–438. https://doi.org/10.3189/172756406781811790

Mériguet, Z., Oddone, A., Le Guen, D., Pollina, T., Bazile, R., Moulin, C., Troublé, R., Prakash, M., de Vargas, C., & Lombard, F. (2022). Basin-Scale Underway Quantitative Survey of Surface Microplankton Using Affordable Collection and Imaging Tools Deployed From Tara. *Frontiers in Marine Science*, *9*. https://doi.org/10.3389/fmars.2022.916025

Muench, R. D. (1971). The Physical Oceanography of the Northern Baffin Bay Region. *Baffin Bay, North Water Project, Scientific Report*, *1*.

Münchow, A., Falkner, K. K., & Melling, H. (2015). Baffin Island and West Greenland Current Systems in northern Baffin Bay. *Progress in Oceanography*, *132*, 305–317. https://doi.org/10.1016/j.pocean.2014.04.001

Olson, R. J., Shalapyonok, A., Kalb, D. J., Graves, S. W., & Sosik, H. M. (2017). Imaging FlowCytobot modified for high throughput by in-line acoustic focusing of sample particles. *Limnology and Oceanography: Methods*, *15*(10), 867–874. https://doi.org/10.1002/lom3.10205

Onarheim, I. H., Eldevik, T., Smedsrud, L. H., & Stroeve, J. C. (2018). Seasonal and Regional Manifestation of Arctic Sea Ice Loss. *Journal of Climate*, *31*(12), 4917–4932. https://doi.org/10.1175/JCLI-D-17-0427.1

Orenstein, E. C., Ayata, S.-D., Maps, F., Becker, É. C., Benedetti, F., Biard, T., de Garidel-Thoron, T., Ellen, J. S., Ferrario, F., Giering, S. L. C., Guy-Haim, T., Hoebeke, L., Iversen, M. H., Kiørboe, T., Lalonde, J.-F., Lana, A., Laviale, M., Lombard, F., Lorimer, T., Irisson, J.-O. (2022). Machine learning techniques to characterize functional traits of plankton from image data. *Limnology and Oceanography*, *67*(8), 1647–1669. https://doi.org/10.1002/lno.12101

Paranjape, M. A. (1987). Grazing by microzooplankton in the eastern Canadian arctic in summer 1983. *Marine Ecology. Progress Series (Halstenbek)*, *40*(3), 239–246. https://doi.org/10.3354/meps040239

Perovich, D. K., Light, B., Eicken, H., Jones, K. F., Runciman, K., & Nghiem, S. V. (2007). Increasing solar heating of the Arctic Ocean and adjacent seas, 1979–2005: Attribution and role in the ice-albedo feedback. *Geophysical Research Letters*, *34*(19). https://doi.org/10.1029/2007GL031480

Pesant, S., Legendre, L., Gosselin, M., Smith, R., Kattner, G., & Ramseier, R. (1996). Size-differential regimes of phytoplankton production in the Northeast Water Polynya (77°-81°N). *Marine Ecology Progress Series*, *142*, 75–86. https://doi.org/10.3354/meps142075

Pollina, T., Larson, A. G., Lombard, F., Li, H., Le Guen, D., Colin, S., de Vargas, C., & Prakash, M. (2022). PlanktoScope: Affordable Modular Quantitative Imaging Platform for Citizen Oceanography. *Frontiers in Marine Science*, *9*. https://doi.org/10.3389/fmars.2022.949428

Ramanathan, V., Cicerone, R. J., Singh, H. B., & Kiehl, J. T. (1985). Trace gas trends and their potential role in climate change. *Journal of Geophysical Research: Atmospheres*, *90*(D3), 5547–5566. https://doi.org/10.1029/JD090iD03p05547

Rose, J. M., & Caron, D. A. (2007). Does low temperature constrain the growth rates of heterotrophic protists? Evidence and implications for algal blooms in cold waters. *Limnology and*

Oceanography, *52*(2), 886–895. https://doi.org/10.4319/lo.2007.52.2.0886

Sakshaug, E., & Slagstad, D. (1991). Light and productivity of phytoplankton in polar marine ecosystems: A physiological view. *Polar Research*, *10*(1), 69–86. https://doi.org/10.3402/polar.v10i1.6729

Schmidt, D. N., Lazarus, D., Young, J. R., & Kucera, M. (2006). Biogeography and evolution of body size in marine plankton. *Earth-Science Reviews*, *78*(3), 239–266. https://doi.org/10.1016/j.earscirev.2006.05.004

Schmoker, C., Hernández-León, S., & Calbet, A. (2013). Microzooplankton grazing in the oceans: Impacts, data variability, knowledge gaps and future directions. *Journal of Plankton Research*, *35*(4), 691–706. https://doi.org/10.1093/plankt/fbt023

Serreze, M. C., Barrett, A. P., Stroeve, J. C., Kindig, D. N., & Holland, M. M. (2009). The emergence of surface-based Arctic amplification. *The Cryosphere*, *3*(1), 11–19. https://doi.org/10.5194/tc-3-11-2009

Sherr, E. B., & Sherr, B. F. (1993). Preservation and Storage of Samples for Enumeration of Heterotrophic Protists. I *Handbook of Methods in Aquatic Microbial Ecology*. CRC Press.

Sherr, E. B., & Sherr, B. F. (2007). Heterotrophic dinoflagellates: A significant component of microzooplankton biomass and major grazers of diatoms in the sea. *Marine Ecology Progress Series*, *352*, 187–197. https://doi.org/10.3354/meps07161

Sherr, E. B., Sherr, B. F., & Hartz, A. J. (2009). Microzooplankton grazing impact in the Western Arctic Ocean. *Deep Sea Research Part II: Topical Studies in Oceanography*, *56*(17), 1264–1273. https://doi.org/10.1016/j.dsr2.2008.10.036

Shindell, D., & Faluvegi, G. (2009). Climate response to regional radiative forcing during the twentieth century. *Nature Geoscience*, *2*(4), 294–300. https://doi.org/10.1038/ngeo473

Simo-Matchim, A.-G., Gosselin, M., Blais, M., Gratton, Y., & Tremblay, J. É. (2016). Seasonal variations of phytoplankton dynamics in Nunatsiavut fjords (Labrador, Canada) and their relationships with environmental conditions. *Journal of Marine Systems*, *156*, 56–75. https://doi.org/10.1016/j.jmarsys.2015.11.007

Sournia, A. (1982). Form and Function in Marine Phytoplankton. *Biological Reviews*, *57*(3), 347–394. https://doi.org/10.1111/j.1469-185X.1982.tb00702.x

Steffen, K. (1985). Warm water cells in the North Water, Northern Baffin Bay during winter. *Journal of Geophysical Research: Oceans*, *90*(C5), 9129–9136. https://doi.org/10.1029/JC090iC05p09129

Steinacher, M., Joos, F., Frölicher, T. L., Bopp, L., Cadule, P., Cocco, V., Doney, S. C., Gehlen, M., Lindsay, K., Moore, J. K., Schneider, B., & Segschneider, J. (2010). Projected 21st century decrease in marine productivity: A multi-model analysis. *Biogeosciences*, *7*(3), 979–1005. https://doi.org/10.5194/bg-7-979-2010

Stevens, C. J., Deibel, D., & Parrish, C. C. (2004). Copepod omnivory in the North Water Polynya (Baffin Bay) during autumn: Spatial patterns in lipid composition. *Deep Sea Research Part I: Oceanographic Research Papers*, *51*(11), 1637–1658. https://doi.org/10.1016/j.dsr.2004.07.011

Tang, C. C. L., Ross, C. K., Yao, T., Petrie, B., DeTracey, B. M., & Dunlap, E. (2004). The circulation, water masses and sea-ice of Baffin Bay. *Progress in Oceanography*, *63*(4), 183–228. https://doi.org/10.1016/j.pocean.2004.09.005

Taylor, A. H., Allen, J. I., & Clark, P. A. (2002). Extraction of a weak climatic signal by an ecosystem. *Nature*, *416*(6881), 629–632. https://doi.org/10.1038/416629a

Ting, M., Kushnir, Y., Seager, R., & Li, C. (2009). Forced and Internal Twentieth-Century SST Trends in the North Atlantic. *Journal of Climate*, *22*(6), 1469–1481. https://doi.org/10.1175/2008JCLI2561.1

Tremblay, J. É., Gratton, Y., Carmack, E. C., Payne, C. D., & Price, N. M. (2002). Impact of the large-scale Arctic circulation and the North Water Polynya on nutrient inventories in Baffin Bay. *Journal of Geophysical Research: Oceans*, *107*(C8), 26-1-26–14. https://doi.org/10.1029/2000JC000595

Tremblay, J. É., Gratton, Y., Fauchot, J., & Price, N. M. (2002). Climatic and oceanic forcing of new, net, and diatom production in the North Water. *Deep Sea Research Part II: Topical Studies in Oceanography*, *49*(22), 4927–4946. https://doi.org/10.1016/S0967-0645(02)00171-6

Tremblay, J. É., Hattori, H., Michel, C., Ringuette, M., Mei, Z.-P., Lovejoy, C., Fortier, L., Hobson, K. A., Amiel, D., & Cochran, K. (2006). Trophic structure and pathways of biogenic carbon flow in the eastern North Water Polynya. *Progress in Oceanography*, *71*(2), 402–425. https://doi.org/10.1016/j.pocean.2006.10.006

Utermöhl, H. (1958). Zur Vervollkommnung der quantitativen Phytoplankton-Methodik: Mit 1 Tabelle und 15 abbildungen im Text und auf 1 Tafel. *Internationale Vereinigung für Theoretische und Angewandte Limnologie: Mitteilungen*, *9*(1), 1–38. https://doi.org/10.1080/05384680.1958.11904091

Vaquer-Sunyer, R., Duarte, C. M., Santiago, R., Wassmann, P., & Reigstad, M. (2010). Experimental evaluation of planktonic respiration response to warming in the European Arctic Sector. *Polar Biology*, *33*(12), 1661–1671. https://doi.org/10.1007/s00300-010-0788-x

Winton, M. (2006). Amplified Arctic climate change: What does surface albedo feedback have to do with it? *Geophysical Research Letters*, *33*(3). https://doi.org/10.1029/2005GL025244

Yamamoto-Kawai, M., McLaughlin, F. A., Carmack, E. C., Nishino, S., Shimada, K., & Kurita, N. (2009). Surface freshening of the Canada Basin, 2003–2007: River runoff versus sea ice meltwater. *Journal of Geophysical Research: Oceans*, *114*(C1). https://doi.org/10.1029/2008JC005000

Yang, E. J., Ha, H. K., & Kang, S.-H. (2015). Microzooplankton community structure and grazing impact on major phytoplankton in the Chukchi sea and the western Canada basin, Arctic ocean. *Deep Sea Research Part II: Topical Studies in Oceanography*, *120*, 91–102. https://doi.org/10.1016/j.dsr2.2014.05.020

Yang, M., & Luo, L. (2008). A rapid auto-focus method in automatic microscope. *2008 9th International Conference on Signal Processing*, 502–505. https://doi.org/10.1109/ICOSP.2008.4697180

Yang, X.-Y., Fyfe, J. C., & Flato, G. M. (2010). The role of poleward energy transport in Arctic temperature evolution. *Geophysical Research Letters*, *37*(14). https://doi.org/10.1029/2010GL043934

Zweng, M. M., & Münchow, A. (2006). Warming and freshening of Baffin Bay, 1916–2003. *Journal of Geophysical Research: Oceans*, *111*(C7). https://doi.org/10.1029/2005JC003093

Aagaard, K., & Coachman, L. K. (1968). The East Greenland Current North of Denmark Strait: Part I. *Arctic*, *21*(3), 181–200. https://doi.org/10.14430/arctic3262

Appendix

Table A1: Observed taxa in the samples collected in northern Baffin Bay between the 13th and 20th of October, 2021.

Protist taxa found in northern Baffin Bay, October 2021
Diatoms
Attheya spp.
Cerataulina spp.
Chaetoceros spp.
Coscinodiscus spp.
Cylindrotheca closterium
Entomoneis spp.
Fragilariopsis spp.
Leptocylindrus spp.
Melosira spp.
Navicula spp.
Pseudonitzchia spp.
Rhizosolenia spp.
Thalassiosira spp.
Dinoflagellates
Amphidinium spp.
Dicroerisma psilonereiella
Gymnodinium spp.
Gyrodinium spp.
Katodinium spp.
Micracanthodinium claytonii
Phalacroma spp.
Protoperidinium spp.
Torodinium spp.
Tripos spp.
Ciliates
Laboea spp.
Leegaardiella spp.
Lohmanniella spp.
Mesodinium spp.
Strombidinopsis spp.
Strombidium spp.

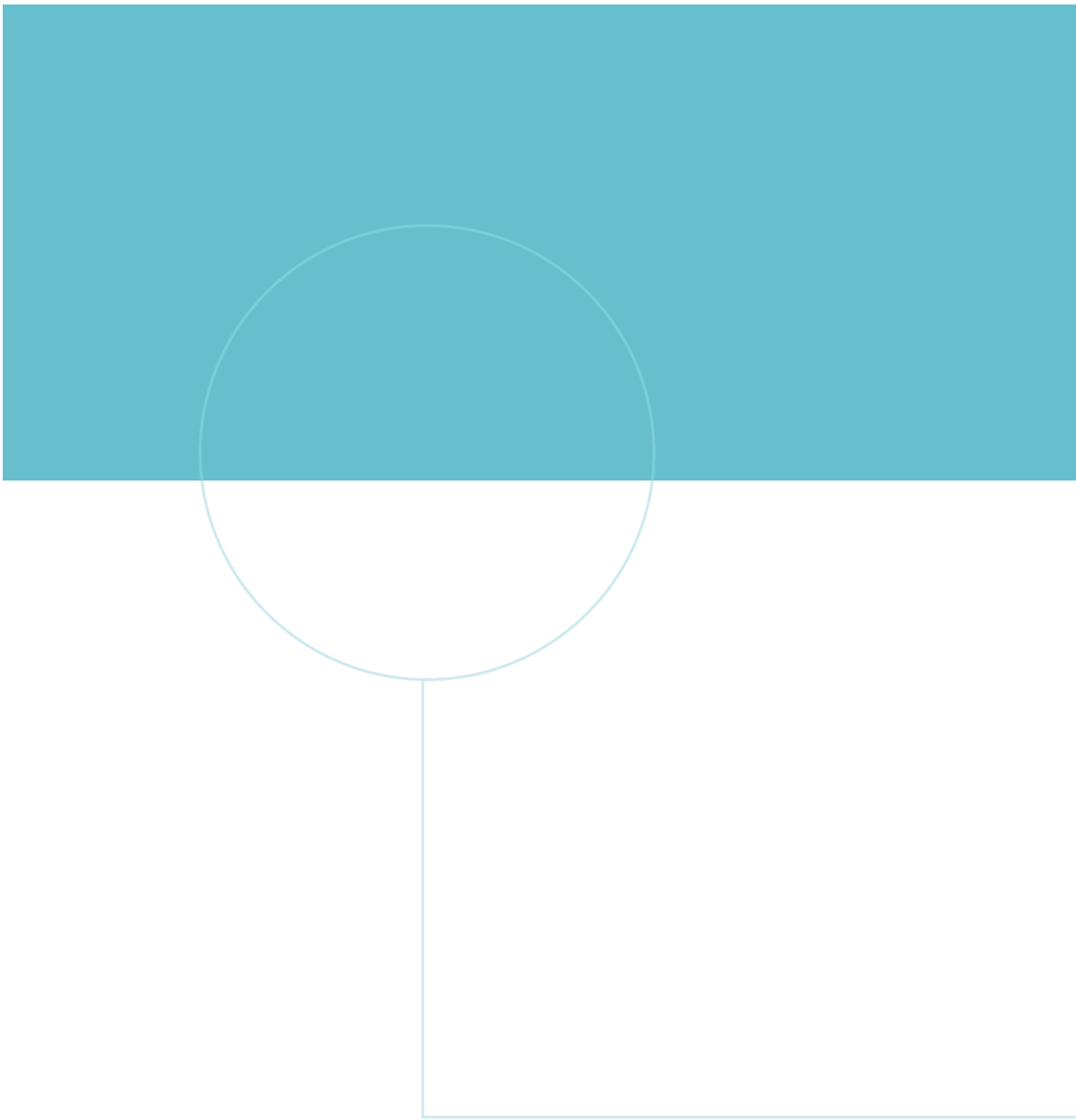

NTNU

Norwegian University of
Science and Technology